HHS Public Access

Author manuscript

Biomaterials. Author manuscript; available in PMC 2019 November 01.

Published in final edited form as:

Biomaterials. 2018 November ; 182: 176–190. doi:10.1016/j.biomaterials.2018.07.062.

Investigation of the effect of hepatic metabolism on off-target cardiotoxicity in a multi-organ human-on-a-chip system.

Carlota Oleaga[a], **Anne Riu**[b], **Sandra Rothemund**[a], **Andrea Lavado**[a], **Christopher W. McAleer**[a,d], **Christopher J. Long**[a,d], **Keisha Persaud**[a], **Narasimhan Sriram Narasimhan**[d], **My Tran**[d], **Jeffry Roles**[a], **Carlos A. Carmona-Moran**[a], **Trevor Sasserath**[d], **Daniel H. Elbrecht**[a,d], **Lee Kumanchik**[a], **Richard L. Bridges**[d], **Candace Martin**[a], **Mark T. Schnepper**[a], **Gail Eckman**[a], **Max Jackson**[a], **Ying I. Wang**[a,e], **Reine Note**[b], **Jessica Langer**[c], **Silvia Teissier**[b], and **James J. Hickman**[a,*]

[a]NanoScience Technology Center, University of Central Florida, 12424 Research Parkway Suite 400, Orlando, FL 32826

[b]L'Oreal Research, and Innovation Division, Aulnay-sous-Bois, France

[c]L'Oreal Research, and Innovation Division, Clark, NJ

[d]Hesperos, Inc., 3259 Progress Dr, Room 158, Orlando, FL 32826

[e]Nancy E. and Peter C. Meinig School of Biomedical Engineering, Cornell University, Ithaca, NY 14853, USA

Abstract

Regulation of cosmetic testing and poor predictivity of preclinical drug studies has spurred efforts to develop new methods for systemic toxicity. Current *in vitro* assays do not fully represent physiology, often lacking xenobiotic metabolism. Functional human multi-organ systems containing iPSC derived cardiomyocytes and primary hepatocytes were maintained under flow using a low-volume pumpless system in a serum-free medium. The functional readouts for contractile force and electrical conductivity enabled the non-invasive study of cardiac function. The presence of the hepatocytes in the system induced cardiotoxic effects from cyclophosphamide and reduced them for terfenadine due to drug metabolism, as expected from each compound's pharmacology. A computational fluid dynamics simulation enabled the prediction of terfenadine-fexofenadine pharmacokinetics, which was validated by HPLC-MS. This *in vitro* platform

[*]**Corresponding Author.** Tel.: +1 407 823 1925; fax: +1 407 882 2819. jhickman@ucf.edu (J.J. Hickman).

Author Contributions

Conceived and designed the experiments: JJH, CO, JL, AR, RN, ST. Performed the experiments: CO, SR, AL, KP, CAC, RLB, TS, DHE, JR. Analyzed the data: CO, SR, CWM, CJL, KP, NSN. Contributed reagents/materials/analysis tools: CJL, MT, CCM, TS, LK, RLB, CM, MTS, GE, MJ, YIW. Wrote the paper: CO, SR, CJL, JJH. Final review: CO, CL, AR, RN, ST, JJH.

Disclosure of Potential Conflict of Interest

The authors confirm that competing financial interests exist but there has been no financial support for this research that could have influenced its outcome. However, JJH and MLS have a potential competing financial interest, in that a company has been formed to market services for types of cells like this in body-on-a-chip devices.

recapitulates primary aspects of the *in vivo* crosstalk between heart and liver and enables pharmacological studies, involving both organs in a single *in vitro* platform. The system enables non-invasive readouts of cardiotoxicity of drugs and their metabolites. Hepatotoxicity can also be evaluated by biomarker analysis and change in metabolic function. Integration of metabolic function in toxicology models can improve adverse effects prediction in preclinical studies and this system could also be used for chronic studies as well.

Keywords

human-on-a-chip; functional readouts; cardiotoxicity; non-invasive; metabolism

Introduction

The regulatory context of March 2013 requires efforts for alternative methods to assess systemic toxicity in the field of cosmetic ingredients, as well as drugs due to the poor human toxicology prediction [1-7]. Cardiovascular and hepatic side effects are the main causes for drugs withdrawn from the market [1], and current models are in many cases failing to accurately predict human outcomes [8, 9]. Moreover, it is well accepted that the liver is the main targeted organ upon exposure to xenobiotics in repeated dose toxicity studies [10]. Conventional *in vitro* assays do not fully represent physiological conditions and xenobiotic metabolism is the missing piece of the puzzle in non-hepatic toxicology assays. There is an urgent need to develop novel human *in vitro* assays offering evaluation of cellular function to improve human prediction upon exposure to drugs and their metabolites [2, 4, 7]. Recent efforts in detecting cardiotoxicity combine the use of human cells and advanced technology including (i) iPSc (induced pluripotent stem cells) derived cardiomyocytes (CM) [11, 12], (ii) the use of high-content functional assay readouts [13-18] and (iii) the ability to separate the cardiac function into electrical and mechanical parameters [19]. The combination of two or more organs in the same model (co-culture) may be essential for understanding the full toxicity profile of a drug (parent compound and metabolites) simultaneously [4].

The liver transforms xenobiotic compounds to improve their elimination from the body; consequently, this transformation may cause changes in drug bioavailability and function. In this sense, the effect of the liver may generate metabolites that are more toxic or more effective than the parent drug. In fact understudied drug metabolism has been implicated in several cases of drug withdrawals [20]. Terfenadine (Seldane®) is a prime example in that it was found to have cardiac side effects after approval but its metabolite fexofenadine did not, and because it has an equal antihistaminic effect as terfenadine is now the marketed drug (Allegra®) [21]. Thus, a system that enables the co-culture of human cardiomyocytes with hepatocytes would be a key development in human-on-a-chip systems to enable the study of induced cardiotoxicity upon hepatic metabolism of compounds as well as hepatic toxicity.

A human *in vitro* system was developed to study cardiotoxicity induced by drugs and their metabolites produced primarily from hepatic cytochrome P450 (CYP) metabolism as well as monitor hepatic viability. This system combines (i) a technology that enables non-invasive electrical and force measurements of cardiac function with (ii) a stable co-culture of human

cardiomyocytes and hepatocytes in a defined, recirculating serum-free medium and (iii) in a pumpless platform that establishes a low volume system to evaluate metabolite formation and its effects. This platform maintained full function of both cell types for 7-28 days under flow. The device was engineered to combine a microfluidic circuit with integrated biological microelectromechanical (BioMEM) chips to ensure maintenance of cellular phenotype and to measure real-time cellular function [19, 22-26]. Two drug models were used for the validation of the system: cyclophosphamide and terfenadine. Cyclophosphamide was selected as a model compound because it is a *non-cardiotoxic parent drug* that generates a *cardiotoxic metabolite* upon liver metabolism, whereas Terfenadine is a *cardiotoxic parent drug* that generates a *non-cardiotoxic metabolite* after hepatic metabolism.

Cyclophosphamide (CP) is an antineoplasic and immunomodulator drug used for a wide spectrum of indications [27-30]. Due to its cardiotoxic side effects [31-37], cyclophosphamide is indicated for patient use only following an individual risk-benefit study. Cardiotoxic side effects of cyclophosphamide usage include hemorrhagic myocarditis, congestive heart failure, depression of left ventricular function, arrhythmia, conduction disorders and QT-interval alterations. The mechanism driving these cardiotoxic events is not yet understood, but findings implicate the production of the metabolite acrolein (ACR) through liver metabolism [27, 30, 38].

Terfenadine (TER) was commercialized in the US market and prescribed until 1997 as an antihistamine before it was withdrawn due to cardiotoxic side effects [21]. In addition to acting as an antihistamine, terfenadine is also a potassium channel blocker, which can prolong the QT-interval and induce *torsade de pointes* and ventricular arrhythmias [39-43]. After terfenadine undergoes metabolism in the liver, the main active metabolite produced is fexofenadine (FEX), which is known to have twenty times less potassium channel blockage activity (relative to the parent terfenadine). Fexofenadine is currently prescribed for the same antihistamine indication as terfenadine had been before it was withdrawn [42, 44, 45].

Cardiotoxicity was measured by tracking cellular functions of beat frequency, conduction velocity, QT-interval, contractile force, daily and non-invasively, after a single acute administration of cyclophosphamide or terfenadine for 72 hours. In addition, hepatic phase I enzymatic activity and cellular viability of both cell types were assessed at day 7. Parent drug (terfenadine) and metabolite (fexofenadine) quantification by HPLC-MS (High pressure liquid chromatography – Mass Spectrophotometry) demonstrated the hepatic clearance of the parent drug and the production of the metabolite. The co-culture of hepatocytes together with cardiomyocytes changed the cardiotoxic profile of the two studied drugs demonstrating the importance of including the hepatic metabolism parameter in the *in vitro* model to better predict human outcomes. A computational model was developed to predict terfenadine and fexofenadine kinetics in the system by combining flow dynamic parameters of the microfluidic system with experimental hepatic metabolic parameters. The model recapitulated terfenadine fate in the heart-liver system as a proof of concept for the device capability to engineer computational prediction. The integration of metabolic function in future toxicology models would improve the prediction of xenobiotics toxicity, providing time and cost savings in the overall safety process. The system described here enables monitoring of cardiac and hepatic function and hepatic biotransformation in serum-

free medium and under flow conditions for the study of acute exposure of parent drugs and their metabolites.

Material and methods

Multi-organ system design and fabrication for functional non-invasive recordings

The heart-liver multi-organ microfluidic device was produced with two outer housing layers of 0.25” thick transparent poly(methyl methacrylate) (McMaster-Carr, Elmhurst, IL, USA) and two 0.5 mm thick gaskets of CultureWell™ silicone (poly(dimethyl siloxane) PDMS) sheet material (Grace Bio-labs, CWS-S-0.5, Bend, OR, USA) to define the flow path and define positions of the bioMEMS chips. The system design was adapted from a 4-organ system previously published [25], with modifications driven by computational fluid dynamics modeling to reduce the size of the system and improve flow characteristics. Designs for each poly(methyl methacrylate) or PDMS component were created in Autodesk Inventor and laser cut using a Versalaser PLS 75W laser cutter (Universal Laser Systems Scottsdale, AZ, USA) (Fig. 1, A). A Zebra® elastomeric electronic connector (FujiPoly Carteret, NJ, USA) was incorporated into the housing to interface the embedded microelectrode array to a custom printed circuit board for electrical measurements. Stainless steel wire electrodes (A-M systems) were embedded in the poly(methyl methacrylate) housing top for electrical stimulation of the cardiac muscle. The versatile microfluidic design contains five chambers for the expansion to additional tissues; in this investigation, only three chambers were used with the layout of the system shown in Fig. 1, A.

Customized multielectrode array (cMEA) chips were designed as two rows of five electrodes each (80 μm diameter, 1000 μm separation, in a total chip size of 1.5 cm × 2 cm) for measuring electrical activity (Fig. 1, B, right). cMEA chips were fabricated from 4” fused silica wafers using standard photolithographic and microfabrication processes at the Cornell Nanoscale Science & Technology Facility (Cornell NanoScience Facility (CNF), Ithaca, NY, USA). After cleaning with a Pirhanha wafer clean, electrodes were fabricated using a liftoff process of electron beam evaporated layers of 10 nm of titanium and 50 nm of platinum. An insulation layer composed of a three-layer stack of silicon oxide/silicon nitride/silicon oxide, each 100 nm thick, was deposited using plasma enhanced chemical vapor deposition and etched with reactive ion etching to expose the electrodes and contact pads. Cantilever (CL) array chips (Fig. 1, B, left), were created for measuring cardiac mechanical function including force and include 32 individual microscale cantilevers (150 μm wide, 735 μm long, 4 μm thick) on each cantilever chip in a total chip size of 1 × 1 cm. Cantilever chips were fabricated from silicon-on-insulator (SOI) wafers using standard photolithographic and deep reactive ion etching techniques at the CNF as previously described [19, 22, 26, 46].

Chemical Modification of cMEA and CL Chips

Chemical modification and patterning using silane chemistry for cell culture were performed and were verified via X-ray photoelectron spectroscopy using previously described methods [19, 24, 46, 47]. The cMEA chips were first modified with a polyethylene-glycol (PEG)-containing self-assembled monolayer, followed by ablation in a U-shaped pattern (150 μm pattern width) covering all ten electrodes in a single path using a 193 nm excimer laser

through a quartz photomask. CL chips were modified with a diethylenetriamine (DETA)-containing silane over the entire cantilever surface to facilitate the adsorption and attachment of fibronectin for controlling cardiomyocyte adhesion on the cantilevers. The cMEA and CL chips were incubated in human fibronectin (10 μg/mL and 50 μg/mL respectively) at 37°C for 30 min. Glass surfaces used for experiments outside the housings were similarly incubated with 10 μg/mL human fibronectin [48].

Cell culture

Cryopreserved human iPSc derived cardiomyocytes (Cellular Dynamic International, CDI, Madison, WI, USA) were plated onto glass coverslips (400 cells/mm^2), cMEA (1000 cells/mm^2) or cantilevers (2,200 cells/mm^2) with HSL2 medium [19, 24, 25] (Supplementary Table 1) and maintained for 7 days before assembly into the housing or performing experimentation, with a half-medium change performed every three days. Cryopreserved human primary hepatocytes (Massachusetts General Hospital (MGH, Boston, MA, USA, lot # Hw36) were plated (1700 cells/mm^2) on collagen coated glass coverslips (60 μg/mL acidified collagen type I for 30 min at 37°C) in MGH medium (Dubelco Modified Eagle Medium (sodium pyruvate, phenol red, glutamine and glucose free) (Thermo Fisher Scientific, A14430-01, Waltham, MA, USA), 10% FBS (Thermo Fisher Scientific, 16000-044, Waltham, MA, USA), 1X antibiotic and antimycotic (Thermo Fisher Scientific, 15240-062, Waltham, MA, USA), 20 mM hydrocortisone (Sigma, H0888, St. Louise, MO, USA), 250 U insulin (Sigma, I9278, St. Louise, MO, USA), 71.4 μg/mL glucagon (Sigma, G2044, St. Louise, MO, USA) and 0.2 ug/mL EGF (Epidermal Growth Factor) (Sigma, E9644, St. Louise, MO, USA)). After a three-hour attachment period, dead or unattached cells were removed by rinsing with 500 μL of MGH medium, followed by complete medium replacement (500 μL). Full media changes were performed every other day for 7 days before assembly into housings or performing static culture experiments.

Experimental design and flow conditions

After 7 days in the cell-specific medium, experiments were performed using serum-free media common between the cardiomyocytes and hepatocytes (HSL2 medium (Hybrid Systems Laboratory 2 medium) for static cultures or HSL3 medium (Hybrid Systems Laboratory 3 medium) [25] for housing-based experiments) (Supplementary tables 1 and 2). Both serum-free media types have been shown to maintain cellular function when co-cultured (Fig. 2 and 3, [25]). Static experiments were done by placing each cell type on a coverslip and both coverslips were placed side by side in a well of a 6-well culture plate with a final volume of 2 mL. Culture conditions and medium exchange were done as described for the microfluidic device. Microfluidic housings were assembled with cardiomyocytes on cMEAs in chamber 3 and on cantilevers in chamber 2, and hepatocytes on coverslips in chamber 1 and secured with stainless steel hex cap screws (Fig. 1, A). The osmolarity of the HSL3 medium in the housing systems was adjusted with sodium chloride to maintain 290 mOsm/Kg throughout the experiment. Medium was recirculated throughout the microfluidic device between the two reservoirs via gravity driven flow generated by a rocker platform (VWR, 12620-906, Radnor, PA, USA) [7, 25, 49-53] inside an incubator maintained at 37°C and 5% CO_2 for up to 28 days. Daily medium changes of 30% of the volume (total volume 2 mL) were performed and collected for further analysis. Throughout the culture period,

cells were imaged and monitored with an inverted phase contrast microscope (Axiovert 200, Carl Zeiss, Oberkochen, Germany) using a 10X objective. Data is presented with respect to the number of days after housing assembly (assembly is Day 0).

Drug treatments were performed on day 4 by the addition of the drug to the reservoir adjacent to the liver compartment (R1, Figure 1). Cardiac function was analyzed by non-invasive measurements on day 4 (before drug addition) and days 5 and 7 (i.e. 24 and 72 h after drug addition). After seven days in the housings, the systems were disassembled for end point CYP enzymatic activity and viability assays.

Urea and albumin secretion quantification

Loss in the ability to produce albumin and urea in hepatocytes is a sign of hepatic damage [54, 55]. Urea and albumin productions were quantified from the supernatant of hepatocytes in monoculture or co-culture with cardiomyocytes with commercial kits (BioAssay Systems (Hayward, CA, USA) and Bethyl Laboratory Inc. (Montgomery, TX, USA), respectively) as described previously [25]. Production is plotted as quantity (μg) of urea, or albumin produced daily normalized to 1×10^6 hepatocytes or normalized to the production on the initial day.

CYP 1A1 and 3A4 enzymatic activity

Maintenance of hepatic p450 activity throughout the co-culture ensured that the model was metabolically competent and inducible p450 activity is important for the study of drug-drug interactions, recommended by the EMA and the FDA [56]. This can also be indicative of hepatic cell health [57]. Cytochrome p450 isoforms 1A1 and 3A4 have been well studied in *in vitro* and *in vivo* models. CYP1A1, despite only accounting for 5% of total drug metabolism, has been well characterized in hepatic *in vitro* models for its relationship with procarcinogens [58-60]. CYP3A4 is one of the main phase I drug metabolizers, and its activity can be induced or inhibited with a variety of compounds, with the potential to create metabolites with toxic properties [61-63]. Phase I 1A1 and 3A4 cytochrome p450 enzymatic activity were measured with a commercial kit (Promega, Madison, WI, USA) at the end point of the experiment (day 7) as described previously [25]. CYP activities are presented as pmol D-Luciferin produced per hour by 1×10^6 hepatocytes, or as normalized to a control.

Immunocytochemistry

Surfaces were fixed and stained with sheep anti-Human Serum Albumin (ABcam ab8940, 1:100, Cambridge, United Kingdom), donkey anti-sheep 568 (Invitrogen A21099, 1:200, Carlsbad, CA, USA) and mounted in Hard Set Mounting with DAPI (Vector laboratories, Burlingame, CA, USA). Images were collected with Axioskop 2 mot plus upright spinning disk confocal microscope (Carl Zeiss, Oberkochen, Germany), with an XCite 120 Fluorescence Illumination system (EXFO) beam and a multi-spectral laser scanning, coupled to Volocity software (Perkin Elmer, Waltham, MA, USA).

Electrical activity measurements

Electrical activity of the cardiomyocytes was measured using a commercially available MEA amplifier (MEA 1040, Multichannel Systems, Reutlingen, BW, Germany) adapted to

the housing system. The cMEA contact pads were connected to the MEA amplifier through a Zebra® elastomeric electrical connector and a custom printed circuit board (Fig. 1, C). The temperature inside the housing was controlled to 37°C by a PID controller (Multichannel Systems, Reutlingen, BW, Germany). Electrical signals were recorded using a commercially available data acquisition software package (MC_Rack, Multichannel Systems, Reutlingen, BW, Germany), with beat frequency quantified from spontaneous recordings (20 s recording period). Cardiomyocytes were electrically stimulated using an STG 1002 stimulator (Multichannel Systems, Reutlingen, BW, Germany) using stimulation parameters described previously in detail [19]. Briefly, a 1 ms bipolar pulse (600-1000 mV) was applied to an individual electrode at increasing frequencies from 0.5 Hz to 4 Hz to control the origin of the conduction path to measure conduction velocity. The minimum interspike interval (mISI, a QT-interval analog) was measured from the data obtained from the frequency sweep, as in [19]. Data analysis was performed in Clampfit 10.3 (Molecular Devices, San Jose, CA, USA), and to measure the electrical parameters of conduction velocity, QT-interval and spontaneous beat frequency. Changes over time are presented as values relative to measurements taken on day 4 (immediately before drug addition) and are compared to control conditions (no drug treatment). For static cultures on coverslips, cardiac beat frequency was quantified microscopically by timing the period required to complete ten contractions and dividing by the number of intervals.

Force measurements

Cardiac force was quantified on cantilevers inside the system using a previously described optical detection system which measures the deflection of the cantilever in direct response to the force exerted by the contracting cardiomyocytes [19, 25, 26, 64]. Cardiomyocyte contraction on cantilevers was induced with electrical stimulation (4V biphasic square wave 0.1 ms in duration at 1 Hz) via embedded stainless steel electrodes using an isolated pulse stimulator (A-M Systems, Sequim, WA, USA). Data analysis was performed using custom peak detection software written in Python to determine peak frequency and average peak amplitude. The amplitudes of the voltage output of the laser detection system in response to cardiomyocyte contraction are directly related to force via Stoney's equation as described previously [64]. Data is presented as detector voltage (μV) or normalized to the contractile force on day 4 (immediately before drug addition) and then compared to control conditions (no drug treatment).

Viability assay

Cell viability was measured after 48 h of drug incubation in monocultures, and the day of disassembly for the flow systems (day 7) using an MTT assay, following [25]. Cardiac cell viability of the flow systems was evaluated using 10% alamarBlue® solution in culture medium (Thermo Fisher Scientific, DAL1100, Waltham, MA, USA) on day 7 of the experiment with a 24h incubation at 37°C. Conversion of the alamarBlue® w as measured with a Synergy HT plate reader and KC4 software (Excitation 530 nm; Emission 590 nm, Winooski, VT, USA). The viability results are presented relative to the control (untreated or incubated with vehicle).

Selected drugs

Two drugs and their selected metabolites were studied for their effects on cardiomyocytes and hepatocytes in the system and in monocultures. Stock solutions of cyclophosphamide (Sigma, 29875, St. Louise, MO, USA) and acrolein (Sigma, 4S8501, St. Louise, MO, USA) were diluted in water; terfenadine (Sigma, T9652, St. Louise, MO, USA) and fexofenadine (Sigma, F9427, St. Louise, MO, USA) were diluted in DMSO. Stock solution concentrations in DMSO were selected such that the DMSO concentration in culture was kept ≤ 0.5% after drug addition. Vehicle controls of water or DMSO were used as control conditions for the respective drugs.

Drug determination and quantification with HPLC-MS

Drug concentrations were determined using an LCMS system consisting of an Agilent Technologies 1100 HPLC interfaced to an Agilent 6490 Triple Quadrupole Mass Spectrometer (Santa Clara, CA, USA). All drugs were separated using gradient elution methodology on a C18 phase (Agilent Zorbax Eclipse Plus, 4.6 mm, 100 mm length, 3 μm particle diameter, Santa Clara, CA, USA) with binary mobile phase (gradient of 30% 20 mM ammonium formate in water and 70% acetonitrile to 70%/30%). Samples (50 μL) were diluted with acetonitrile (1:4 v/v) and centrifuged to precipitate proteins after addition of the internal standard. The MS equipped with an electrospray source and used in positive ion mode and Multiple Reactive Monitoring (MRM) with nitrogen used for collision induced dissociation. The reported quantitation limits corresponded to a signal to noise ratio of approximately 10. The methodology described below was adapted from these publications [65, 66].

Terfenadine and fexofenadine were analyzed with an internal standard, propranolol (Sigma, 40543, St. Louis, MO, USA). For terfenadine, fexofenadine and propranolol quantification, the MRM (parent/daughter) transitions used were m/z 472 to 436, 502 to 466, and 260 to 116, respectively. The collision energy parameter was set to 24 (terfenadine and fexofenadine) and 16 for propranolol. Dwell time was set to 50 ms and acceleration voltage to 5 V for each of these three species. The limits of quantitation were 1.25 nM for both terfenadine and fexofenadine.

Computational simulation of fluid dynamics and drug metabolism in the Heart-Liver system

A transient model for gravity driven flow on the rocking system previously developed with computational fluid dynamics software (CFD, CFD-ACE+ (ESI Group, Paris, France) [25] was used to compute the shear stresses in each of the organ chambers (Supplementary Figure 1), with shear stresses below 0.05 dynes/cm^2 (within acceptable physiologic ranges [25]). These shear stresses are high enough to produce induced changes to mimic *in vivo* behavior without causing damage [67, 68]. Concentration-time profiles were determined from experimental mixing experiments using fluorescent dyes to track mass transport. The mixing profile of compounds in the system for multiple days was modeled using an exponential growth function involving a time constant and was fit to the experimental mixing data. The renewal of compound during the daily 30% medium change was incorporated into the model every 24 hours. Adsorption of compounds to the system was

measured via HPLC over 24 hours in systems not containing tissues and fit to a second exponential decay function. Mixing and adsorption were convolved numerically to predict the concentration of drug in the device following adsorption losses and accounting for mixing (Fig. 9, A).

Conversion of a parent drug to a metabolite was modeled using a two tier process to incorporate both the decrease in parent drug concentration in the system due to uptake by the hepatocytes and the increase in metabolite concentration due to conversion of the parent to the metabolite. To decouple metabolic rate constants from the effects of flow and adsorption, these Michaelis-Menten metabolic rate constants for the conversion of terfenadine to fexofenadine were determined using hepatocyte cultures in static well plates with administered terfenadine concentrations of 1-100 μM. Conversion over 24 hours of terfenadine to fexofenadine was measured via HPLC-MS. The two tier metabolism model incorporated Michaelis-Menten kinetics for the parent drug being transported into the cell, with constants determined from the concentration of the drug in the medium, and the conversion of the intracellular drug to the metabolite, and release to the medium. Using the measured concentrations of both terfenadine and fexofenadine in the wells, and applying a conservation of mass constraint, the uptake constants of terfenadine into the cells and the conversion rate constants inside the cells were calculated.

The Michaelis-Menten constants we obtained from incubation the drugs in hepatocytes in monoculture and static & flow conditions and quantifications of the metabolite. The Km values computed for the parent compound conversion to metabolite (Km = 15 μM) fall in the range found in the literature [69-71]. Each of these functions; mixing due to sinusoidal rocking, mixing modified for medium changes, adsorption, transport into the cell, and metabolism—were combined numerically in MathWorks' MATLAB (Natick, MA, USA) using an iterative scheme along with the acute dosing of the drug to predict the parent and metabolite concentration in the organ chambers over 72 h after dosing.

Statistical methods

Numerical data is expressed as the mean ± SE of a minimum of three independent experiments. Changes between two conditions (i.e. control vs. condition) were evaluated with unpaired two-tailed Student's t-Test. For time series, one- and two-way ANOVA followed by Dunnet post hoc analysis were used to evaluate the effects of changes in time and condition. All statistical analyses were performed with Microsoft Excel, except for the two-way ANOVA performed in Sigma Plot 12.5 (Systat Software, Inc. Chicago, IL, USA) and differences with p-values < 0.08 were taken as statistically significant.

Results

Static human cardiomyocyte and hepatocyte co-culture characterization in serum-free medium.

The co-culture of human cardiomyocytes and hepatocytes on coverslips in 6-well plates with HSL2 serum-free medium (2 mL) were characterized. Representative morphology images of cardiomyocytes (left) and hepatocytes (right) after 7 days in mono-culture (top) or in

coculture (bottom) (Fig. 2, A) indicated no morphological differences between cells in co-cultures and those in respective mono-cultures, nor was viability different between the two conditions at day 7 (Fig. 2, B). The cardiac spontaneous beat frequency was measured daily (Fig. 2, C) in the mono-culture condition, and increased (18 %) in the presence of the hepatocytes. The hepatic metabolic profile remained unaffected by the presence of cardiomyocytes, as measured by production of albumin (Fig. 2, D and E), urea (Fig. 2, E) and CYP1A1 and CYP3A4 enzymatic activities (Fig. 2, E) at day 7. Phenotypic variances among different hepatic donors were also evaluated using CYP activity to determine if the presence of the cardiomyocytes would affect phase I metabolism. Cardiomyocytes were further co-cultured with HepG2/C3A and human primary hepatocytes from a second donor (MGH, lot HR-5) for 7 days. No significant differences were observed in CYP activity when comparing mono-culture to co-culture (data not shown). Overall, cardiomyocytes and hepatocytes maintained their morphology and function in the coculture in the HSL2 serum-free medium over a 7-14 day period.

Characterization of the recirculated heart and liver co-culture platform.

Human cardiomyocytes were seeded on custom MEAs for electrical activity measurements and cantilever chips for mechanical activity, and cultured together with hepatocytes on glass coverslips in the HSL system containing serum-free medium (2 mL HSL3). The recirculation of the medium in the platform was enabled by a pumpless gravity driven system controlled by a rocker platform located inside a cell culture incubator. The oscillatory rocking maintained adequate mixing of nutrients and enabled sufficient gas exchange through the reservoirs. Modeling of the flow dynamics in the system by mimicking the oscillatory profile from the sinusoidal rocking was used to keep the maximum shear stress below 0.05 dynes/cm^2 at the bottom wall of each chamber where the cells were located (Supplementary Figure 1).

Representative images of both patterned cardiomyocytes on custom MEAs (Fig. 3, A) and cantilevers (Supplementary Figure 2) alone or in the presence of the hepatocytes (Fig. 3, B) indicated good morphology after 7 days under flow in the microfluidic system. Cardiac electrical and contractile function was measured non-invasively in the HSL systems, with or without hepatocytes, over 7 days. None of the measured cardiac parameters (conduction velocity, mISI (equivalent to QT-interval), beat frequency and force) were affected by time (all $p>0.08$). Spontaneous beat frequency, mISI (or QT-interval) and contractile force parameters were the same in the presence or absence of hepatocytes (around 0.5 Hz, 1.2 s, and 13 μV, respectively) (Fig. 3, C). Only the cardiac conduction velocity showed a maximum of 0.05 m/s decrease at day 6 in the presence of hepatocytes (24.57 ± 4.75% reduction) (Fig. 3, C). Hepatic CYP1A1 and 3A4 activities were stable over time in the presence of cardiomyocytes with an activity of 0.3 ± 0.1 and 0.8 ± 0.1 pmol D-Luc/h/10^6 cells, respectively (Fig. 3, D). As a proof of concept, the co-culture system was further maintained for 28 days and daily analysis of cardiac and hepatic functions confirmed the viability of the system over this extended period of time (Supplementary Figure 3).

Toxicity evaluation of terfenadine and cyclophosphamide and their metabolites in mono-culture

A cyclophosphamide dose response profile (50-9000 μM), measured separately in cardiomyocytes and hepatocytes, corroborated the predominately non-cardiotoxic profile of the drug on cardiomyocytes at the therapeutic plasma range (2-250 μM [27-30]). However, cyclophosphamide affected cardiac beat frequency at the highest concentration (9000 μM) (Fig. 4, A, left). The contribution of the CYP 3A4 in the metabolism of cyclophosphamide caused a positive and dose-dependent enzyme induction starting at 500μM in the hepatocytes (Fig. 4, B, left). The control experiment with the cyclophosphamide metabolite, acrolein (30-500 nM), did induce cardiotoxicity by affecting the cellular viability, and the beat frequency at, concentrations lower than the human plasma concentrations reported after cyclophosphamide administration (low micro molar range) [30, 72] (Fig. 4, A, right). In the hepatocyte mono-culture, no CYP induction was observed, but a significant loss of cell viability was quantified with increasing concentration of acrolein (Fig. 4, B, right).

A dose-response study of terfenadine (1-10 μM) on cardiomyocytes in mono-cultures corroborated the cardiotoxic profile of the drug. The measured effective concentration range included the therapeutic human plasma concentrations (0.02-3 μM) and was also used in previous *in vitro* studies [11,41, 73, 74]. Terfenadine affected cardiac function before viability, with a strong effect in contractile activity observed at 1 μM (80.0 ± 8.4% decrease in beat frequency), while cell viability was not affected until higher concentrations (20.6 ± 12.6% at 5 μM and 44.7 ± 11.9% at 10 μM) (Fig. 5, A, left). The metabolite fexofenadine (1-10 μM) produced negligible toxicity in the cardiomyocytes, with functional parameters remaining within 18% of the control, and cell viability decreasing by less than 19% (Fig. 5, A, right). No significant changes were observed in the hepatic viability upon the terfenadine, or fexofenadine incubations. Moreover, although the CYP 3A4 is known to participate in the metabolism of terfenadine [69, 75, 76], there was no induction, as it has been observed above for cyclophosphamide (Fig. 5, B and Fig. 4, B).

Pharmacokinetic study of the integrated system for drug metabolism

The flow systems with cardiomyocytes with or without hepatocytes were challenged with acute administration of cyclophosphamide (9 mM) and terfenadine (10 μM). Cardiac function was monitored before and after (24 and 72 h) the addition of the drug, and cell morphology was imaged the same days of measurements. Hepatic metabolism was measured indirectly by cardiac function changes upon drug treatment over time. The viability of both cell types, and CYP activities, were analyzed as endpoint indicators after the disassembly of the systems on day 7. The concentrations selected for cyclophosphamide and terfenadine aimed to affect function but not cell viability in the fluidic system. We used the previous dose-response results in the static mono-cultures and the physicochemical characteristics of the drugs to account for adsorption of the hydrophobic drugs onto the housing material. The HSL systems have the advantage that the bulk of the system is not PDMS, which is known to adsorb hydrophobic drugs [77, 78]. Instead, the bulk of the housing system is a thermoplastic polymer, which exhibits less adsorption of hydrophobic drugs than PDMS [79]; however, some adsorption occurs due to the PDMS gasket material.

Cyclophosphamide (9 mM) significantly affected the cardiac function (electrical and mechanical) in the presence of hepatocytes (Fig. 6, A-D-green). Cardiac conduction velocity, spontaneous beat frequency and contractile force were strongly reduced by 62.2 ± 21.7%, 93.2 ± 6.6% and 80.8 ± 10.1%, respectively within the first 24 h after cyclophosphamide (9 mM) addition (Fig. 6, A, B and D). An increased in the mISI of 71.3 ± 39.3% was also observed (Fig. 6, C), indicating a QT-interval prolongation. Without the liver compartment in the system, cyclophosphamide still affected the contractile force at 9 mM with a 61.2 ± 18.4% decrease (Fig. 6, D), however the cardiac function recovered after 72 h, while in the presence of the hepatocytes, the contractile force remained compromised with 50.4 ± 9.3% decrease (Fig. 6, D). These results, suggested a potential metabolic activation inducing cardiotoxicity. A complete recovery of the electrical function and a partial recovery of the contractile force suggest that the effect of the metabolite was reduced after 72 h. As expected CYP3A4 activity was strongly induced in a dose-dependent manner with cyclophosphamide without any cell cytotoxicity, as previously observed in the mono-cultures (Fig. 8, A). Under flow conditions, 9 mM cyclophosphamide exposure induced an increase in cardiomyocytes viability of 37.7 ± 12.8% with hepatocytes and 22.6 ± 6.2 % without hepatocytes (Fig. 6, E).

Terfenadine (10 μM) significantly affected the cardiac function (electrical and mechanical) in the absence of the hepatocytes (Fig. 7, A-D-red/grey). Indeed, 25.0 ± 10.5%, 42.7 ± 10.6% and 65.0 ± 12.0% decrease in cardiac conduction velocity (Fig. 7, A) spontaneous beat frequency (Fig. 7, B) and contractile force (Fig. 7, D) were observed after 24 h of terfenadine exposure in the absence of hepatocytes, respectively. The mISI interval increased (117 ± 39%) indicating QT-interval prolongation (Fig. 7, C). With hepatocytes in the system, no significant functional changes were observed except contractile forces (Fig. 7, D) which were still affected by a 43.2 ± 15.0% decrease upon terfenadine treatment. Both the electrical and the contractile parameters recovered after 72 h and no significant changes were observed in viability at this concentration (Fig. 7, E). There were no significant changes quantified for CYP1A1 and CYP3A4 activities, together with no changes in hepatocyte viability upon 10 μM terfenadine treatment, as was previously observed in the mono-culture study (Fig. 8, B).

Pharmacokinetic profile of terfenadine in the heart-liver system

In the system, drugs were administered through the reservoir closest to the liver chamber (chamber 1, R1) to mimic first pass metabolism, and the effects were evaluated in silico at 24 and 72 h after administration. Distribution of the drugs in the system depended on the flow dynamics, the adsorption rate into the material of the system, the rate of transport into the cells and the media exchange performed daily in the system. A numerical model that incorporated each of these components was created from experimental data and CFD modeling. The mixing profile for each drug was computed by integrating the flow dynamics previously modeled with experimentally generated data of the drugs in the HSL system without cells. The kinetic profile of the drugs in the HSL system depended on the distribution of the drugs and the metabolic rate of the hepatocytes. The distribution and metabolism of terfenadine, as well as the metabolite production rate in the heart-liver system, were modeled. The combination of low rates of metabolism and adsorption for

cyclophosphamide resulted in the selection of terfenadine over it for modeling purposes. However, experimentally derived concentrations of cyclophosphamide and acrolein confirmed expected concentrations in the system. Modeling results were compared to experimental measurements of the prodrug and metabolite concentrations in the system at different time points using HPLC-MS. Terfenadine is a very hydrophobic compound; as a result, 98% of the drug (10 μM) was lost after 24 h in the system due to adsorption. It is known that terfenadine may accumulate in the hepatocytes, [80], thus kinetic parameters of transport were considered in the modeled profile as part of the two-tier process of metabolism, in which 1) the terfenadine entered the cell and 2) the terfenadine in the cell was converted to fexofenadine. These parameters were created from concentration-time profiles in the medium for both terfenadine and fexofenadine. Fexofenadine was detected only in the HSL systems that contained hepatocytes, providing a positive indication of terfenadine metabolism to fexofenadine. The computational model of terfenadine kinetics was close to the experimental measurements. The mean difference in the prediction versus experimental measurements at 24, 48, and 72 hours was 23.7 ± 33.1%, which is considerably smaller relative to the total changes in concentration in the system due to adsorption on the plastic, metabolism, and elimination (from medium exchange) (Fig. 9, B).

Discussion

Human-on-a-chip systems enable the co-culture of cells from various organs under the same blood surrogate to reproduce several aspects of the *in vivo* environment [4, 25]. In this context, the liver plays an important role in the metabolism of xenobiotics and although hepatic metabolism is thoroughly studied in toxicological investigations, the study of hepatic function together with other organs is normally delayed until later. The incorporation of a liver representative in the *in vitro* system enables a full systemic efficacy and toxicity profile (parent drug and metabolites) [2, 5, 81, 82]. *In vitro* co-culture systems with hepatocytes and other cell types for studying drug toxicity upon hepatic metabolism have been investigated before under static conditions with rat hepatic microsomal fractions [30] and human primary hepatocytes [83, 84], as well as under flow with different microfluidic approaches with hepatic cell lines [85-87], [88], [89] and [25]. However, this is the first study combining human primary hepatocytes and iPSc derived cardiomyocytes, serum-free conditions, non-invasive analysis of cellular function, quantification of drug metabolism and PK/PD analysis in a multi-organ system.

Cardiotoxicity is a major recurrent side effect during preclinical drug development [3], and unfortunately aftermarket release [2], which can trigger the withdrawal for human use [2]. The recent commercialization of iPSc derived cardiomyocytes has enabled advances in cardiotoxicity prediction [11, 12]. Engineering technology applied to the cardiomyocyte cultures has enabled the quantification of cardiac function [13-19, 24, 25] and the possibility of high-throughput screening [6, 13, 15, 16, 18, 19]. Cardiotoxic events are often driven by hepatic transformation of drugs [83, 90, 91], thus the incorporation of a liver module in a cardiac *in vitro* system enables the recreation of a more realistic scenario for drug development studies [2, 5, 81, 82].

A previous study from our group demonstrated the co-culture of cardiomyocytes and hepatocytes, in addition to neurons and skeletal muscle, under flow in a defined serum-free medium for 14 days [25]. In this work, human primary hepatocytes substituted for the previously used HepG2/C3A cell line. Further characterization of the human co-culture demonstrated the maintenance of cellular function for both cardiomyocytes and hepatocytes for up to 28 days under flow and serum-free conditions (Supplementary Figure 3). The stable co-culture of these two cell types in our system were in agreement with the supportive [92-95] and protective [96] effects known between the heart and the liver organs previously described in the literature. In addition, the function of hepatocytes from different sources and with different phenotypes was not altered by the presence of cardiomyocytes in this platform. In order to reduce data variability, the main study was done with a single donor of human primary hepatocytes.

The housing was designed to be reconfigurable which enables the co-culture of many different organs. The cantilever chip used for the measurement of contractile force was previously designed and validated [19, 22, 26]. A detection system for non-invasive contractile force measurements was designed using laser beam deflection from the tip of the cantilever [19, 26, 64] to access the chip inside the housing and to allow an automated calibration of each individual cantilever. The design and fabrication of the custom MEA used in this work allowed for the reduction of the chip size in order to fit in the housing and to enable non-invasive recordings. With this non-invasive technology, cardiac parameters such as conduction velocity, beat frequency, QT-interval, (or mISI) and force can be tracked on a daily basis.

Characterization of cardiac function in the housing indicated no changes upon co-culture with hepatocytes, except for conduction velocity (24.6 ± 6.3% average reduction, $p=0.0006$). We postulate that the small, but significant, changes observed could be a side effect of reducing the nutrient/cell ratio or to an organ crosstalk regulation [97]. In the static co-culture characterization study, there was a difference in beat frequency upon the presence of hepatocytes ($p=0.049$). However, beat frequency remained stable with hepatocytes in the housing, suggesting that the co-culture in the microfluidic housing is more stable and represents a more precise, robust and reproducible quantification method than static co-culture. Basal hepatic 3A4 p450 activity, but not 1A1, was reduced due to the change to HSL3 medium, not due to the introduction of flow (data not included), when we translate the co-culture to the microfluidic system. This change did not affect the ability of the hepatocytes to metabolize the drugs or to respond to inducers of the activity.

In order to validate the heart-liver system, we used the compounds cyclophosphamide and terfenadine. Cyclophosphamide was selected because it is considered a non-cardiotoxic compound that upon liver transformation will generate cardiotoxic metabolites. As expected, in the static monoculture conditions for each cell type, 48 h incubation with cyclophosphamide did not show any effects on cardiomyocytes viability and beat frequency (up to 2 mM) and induced CYP 3A4 enzymatic activity in hepatocytes [30, 98]. The liver transformation of cyclophosphamide generates a wide range of metabolites [37, 99-101] and acrolein has been previously correlated to cyclophosphamide cardiotoxic side effects [27, 30, 38]. In the cardiac mono-culture, acrolein reduced beat frequency and viability at

concentrations of ≥ 300 nM, corresponding to even lower concentrations than the ones detected in plasma for therapeutic levels of cyclophosphamide [30, 72]. In the flow system, cyclophosphamide (9 mM) induced negative changes in the cardiac electrical activity only in the presence of hepatocytes. After 24 h incubation, conduction velocity, beat frequency and contractile force dropped significantly by a range of 60-93% ($p=0.04$, $p<0.001$ and $p<0.001$), together with a prolongation of the QT-interval of 71% ($p=0.08$). Changes in beat frequency and QT-interval have been previously reported *in vitro* [12, 33, 102]. The heart-liver system with the protocol used provides two drug elimination pathways: the hepatic clearance and the media exchange (30% exchanged daily). The cardiotoxic effects observed in the first 24h of treatment with cyclophosphamide confirmed hepatic clearance due to metabolites formation. The media changes performed on days 5 and 6 cleared out enough of the metabolites to enable the recovery of the cardiomyocytes during the next 48 h following cyclophosphamide treatment. Although the electrical activity indicated a clear difference in the system with or without hepatic cells, the contractile force was equally sensitive to the prodrug cyclophosphamide (9 mM) or its metabolites. These results suggest that cyclophosphamide, at the highest concentration of 9 mM, caused toxicity in cardiac contractile function before being metabolized which is in accordance with the dose-response performed in static cardiomyocytes showing an effect in the beat frequency at the highest concentration (9 mM). However, at 72 h after the addition of cyclophosphamide into the heart-liver system, the cardiomyocytes still did not recover their contractile function, whereas the cardiac cells in the absence of hepatic cells did. This result confirms the toxicity profile of cyclophosphamide upon hepatic metabolism. The cardiomyocyte viability quantified after 72 h of treatment (day 7) confirmed no observed viability deficits. Interestingly, a significant increase in viability was observed for the cyclophosphamide dosed cardiac cells in the absence ($p=0.03$) or the presence of hepatocytes ($p=0.03$) as compared to the control. This increase was not expected based on the earlier reported studies in which a reduction in the H9c2 cell line viability after 24-48 h incubation with cyclophosphamide (250-500 μM) was shown, but only in the presence of hepatic microsomes [30]. This could be an artifact due to cyclophosphamide (9 mM) interference with the alamarBlue reaction or detection, resulting in an artificial increase value of viability using this assay. Indeed, the increase in cardiac viability was not observed in the mono-culture experiments with cyclophosphamide or the hepatocytes, in which viability was estimated by an MTT assay. Cyclophosphamide, as observed in the mono-culture, induced the hepatic CYP 3A4 activity in the flow system in a dose-dependent manner and without affecting hepatic viability ($p<0.001$).

Terfenadine is a cardiotoxic parent drug that generates a non-cardiotoxic metabolite upon liver transformation according to the literature [41]. The drug is metabolized by CYP3A4 [75], thus the inhibition of this enzyme caused by the interaction with other drugs or compounds may trigger a cardiotoxic effect [74]. In the static monoculture condition, the toxicity of terfenadine was confirmed in cardiomyocytes after 48 h incubation in a dose-dependent manner for beat frequency (80% of beat frequency reduction at 1 μM) and viability (50% of cell death at 10 μM). Previous *in vitro* studies showed cardiotoxicity in the same range of terfenadine concentrations [11,41]. The main metabolite, fexofenadine, is nontoxic in the concentration range studied (from 1 μM to 10 μM). In the flow system, the

presence of the liver protected from the cardiotoxic effect of terfenadine (10 μM) on the electrical parameters (conduction velocity, beat frequency, and QT-interval), but not on the mechanical force. Despite hepatic clearance (metabolic biotransformation), terfenadine impacted the cardiac contractile function. The drug clearance, induced by media exchange, restored cardiac function in both conditions after 72 h, with the exception of the beat frequency. As expected, terfenadine did not affect the hepatocyte viability, and in correlation with the observations made in the hepatic mono-cultures, terfenadine (1-10 μM) did not induce CYP1A1 or CYP3A4 activities.

The heart-liver system indirectly measured hepatic drug metabolism through the evaluation of the cardiac outcome. For validation, the metabolic function of the human primary hepatocytes was directly confirmed by the quantification of the parent drug and metabolite formation in the system. An in silico model that integrated the flow dynamics of the system and the kinetic profile was developed to enable the simulation of the metabolism of terfenadine in the heart-liver system. This model incorporated several forms of removal of the compounds (specifically adsorption, metabolism, and medium changes), which combined provided an in vitro analogue to half-life. The experimentally determined parameters for mixing and adsorption were combined with those for metabolism to create a pharmacokinetic profile in the system. The focus of the current work is on the time period of 1-3 days after drug delivery for both functional measurements and medium concentrations; however, further extensions of the experimental validation for early time points is straightforward for use in studies with shorter-term times of interest. Although the computational model predicted the final concentration of terfenadine, a deviation at the initial time points was observed. This could be attributed to the bioaccumulation of the metabolite in the cell systems. The current model does not account for absorption of compounds post-release from the cell. A second limitation is the modeling of temporal dynamics of binding and re-release of compounds bound to the PDMS in the device, which was determined from experimental observations. Future work intends to include a more complex computational model that addresses the limitations discussed above to ultimately generate an *in silico* platform that could be used to predict the fate of unknown drugs, and together with the integration of a library of cardiotoxic and hepatotoxic drugs built from experimental data in the HSL system, it could predict human outcomes.

Overall, the heart-liver system is a low-cost and easy to use platform that enables human cardiomyocytes and hepatocytes to being co-cultured in a serum-free defined medium under gravitationally induced flow for evaluating cardiotoxicity-dependent drug metabolism. Cyclophosphamide metabolites and terfenadine adversely affected the cardiac function for a period of 24 h followed by recovery. The current technology is able to perform studies that are required for the *in vitro* safety pharmacology preclinical evaluations mandated by the ICH guidelines [8]. Besides the current status of the system, the versatility of the engineered design enables further studies such as the evaluation of other hepatic phenotypes, the use of iPSc derived hepatocytes, the addition of other organs in the co-culture, drug interaction studies, chronic drug exposure and personalized medicine. Furthermore, the system could be used to predict cardiac toxicity of newly developed drugs based on previous physiologically based pharmacokinetic studies performed using the platform.

Conclusions

A novel *in vitro* platform has been developed for the study of cardiotoxicity upon hepatic metabolism. The co-culture of human primary hepatocytes with iPSc derived cardiomyocytes was achieved under serum-free conditions and under flow in a microfluidic platform with stable cellular viability and function for 28 days. The engineering control of the platform for microfluidic design and compatibility with bioMEMS and biologic cultures made possible a non-invasive daily measurement of the cellular functions. This technology allowed the indirect study of the hepatic metabolic function by tracking cardiac function (electrical and mechanical). Two known drugs related to cardiac side effects dependent on hepatic metabolism were used to challenge the system. The heart-liver system was able to predict human cardiac toxicity upon compound transformation through hepatic metabolism, thus this system represents a novel platform that could be used in preclinical studies and a starting point to move towards a more complex human-on-a-chip device.

Supplementary Material

Refer to Web version on PubMed Central for supplementary material.

Acknowledgments

We acknowledge support from the research collaboration and grant from L'Oreal Corporation as well as an NIH SBIR Phase II, grant number UH2TR000516. We thank Maria Stancescu, Aditya Reddy Kolli, Balaji Srinivasan Venkatesh, William McLamb, Vivien Platt, Gregg Legters, Catia Bernabini and Kazi Tasneem for their contribution to the initial phase of this work and Kerry Wilson for assistance in the electrical recordings.

References

[1]. Siramshetty VB, Nickel J, Omieczynski C, Gohlke BO, Drwal MN, Preissner R, WITHDRAWN--a resource for withdrawn and discontinued drugs, Nucleic Acids Res 44(D1) (2016) D1080–6. [PubMed: 26553801]

[2]. Ribas J, Sadeghi H, Manbachi A, Leijten J, Brinegar K, Zhang YS, Ferreira L, Khademhosseini A, Cardiovascular Organ-on-a-Chip Platforms for Drug Discovery and Development, Applied In Vitro Toxicology 2(2) (2016) 82–96. [PubMed: 28971113]

[3]. Cook D, Brown D, Alexander R, March R, Morgan P, Satterthwaite G, Pangalos MN, Lessons learned from the fate of AstraZeneca's drug pipeline: a five-dimensional framework, Nat Rev Drug Discov 13(6) (2014) 419–31. [PubMed: 24833294]

[4]. Esch MB, Smith AS, Prot JM, Oleaga C, Hickman JJ, Shuler ML, How multi-organ microdevices can help foster drug development, Adv Drug Deliv Rev 69–70 (2014) 158–69. [PubMed: 24412641]

[5]. Hutson MS, Alexander PG, Allwardt V, Aronoff DM, Bruner-Tran KL, Cliffel DE, Davidson JM, Gough A, Markov DA, McCawley LJ, McKenzie JR, McLean JA, Osteen KG, Pensabene V, Samson PC, Senutovitch NK, Sherrod SD, Shotwell MS, Taylor DL, Tetz LM, Tuan RS, Vernetti LA, Wikswo JP, Organs-on-Chips as Bridges for Predictive Toxicology, Applied In Vitro Toxicology 2(2) (2016) 97–102.

[6]. Loskill P, Marcus SG, Mathur A, Reese WM, Healy KE, muOrgano: A Lego(R)-Like Plug & Play System for Modular Multi-Organ-Chips, PLoS One 10(10) (2015) e0139587. [PubMed: 26440672]

[7]. Miller PG, Shuler ML, Design and demonstration of a pumpless 14 compartment microphysiological system, Biotechnol Bioeng (2016).

[8]. H.f.b.h. (ICH), ICH Guidelines, 2016 http://www.ich.org/products/guidelines.html.

[9]. Vijayananthan A, Nawawi O, The importance of Good Clinical Practice guidelines and its role in clinical trials, Biomed Imaging Interv J 4(1) (2008) e5. [PubMed: 21614316]

[10]. Vinken M, Pauwels M, Ates G, Vivier M, Vanhaecke T, Rogiers V, Screening of repeated dose toxicity data present in SCC(NF)P/SCCS safety evaluations of cosmetic ingredients, Arch Toxicol 86 (2012) 405–12. [PubMed: 22038139]

[11]. Doherty KR, Talbert DR, Trusk PB, Moran DM, Shell SA, Bacus S, Structural and functional screening in human induced-pluripotent stem cell-derived cardiomyocytes accurately identifies cardiotoxicity of multiple drug types, Toxicol Appl Pharmacol 285(1) (2015) 51–60. [PubMed: 25841593]

[12]. Khan JM, Lyon AR, Harding SE, The case for induced pluripotent stem cell-derived cardiomyocytes in pharmacological screening, Br J Pharmacol 169(2) (2013) 304–17. [PubMed: 22845396]

[13]. Agarwal A, Goss JA, Cho A, McCain ML, Parker KK, Microfluidic heart on a chip for higher throughput pharmacological studies, Lab Chip 13(18) (2013) 3599–608. [PubMed: 23807141]

[14]. Egert U BK, Meyer T, Analysis of Cardiac Myocyte Activity Dynamics with Micro-Electrode Arrays, in: Taketani M BM (Ed.), Advances in Network Electrophysiology, Springer, Singapore, 2006, pp. 274–290.

[15]. Kaneko T, Nomura F, Hamada T, Abe Y, Takamori H, Sakakura T, Takasuna K, Sanbuissho A, Hyllner J, Sartipy P, Yasuda K, On-chip in vitro cell-network pre-clinical cardiac toxicity using spatiotemporal human cardiomyocyte measurement on a chip, Sci Rep 4 (2014) 4670. [PubMed: 24751527]

[16]. Mathur A, Loskill P, Shao K, Huebsch N, Hong S, Marcus SG, Marks N, Mandegar M, Conklin BR, Lee LP, Healy KE, Human iPSC-based cardiac microphysiological system for drug screening applications, Sci Rep 5 (2015) 8883. [PubMed: 25748532]

[17]. Starc V, Schlegel TT, Real-time multichannel system for beat-to-beat QT interval variability, J Electrocardiol 39(4) (2006) 358–67. [PubMed: 16919668]

[18]. Su X, Young EW, Underkofler HA, Kamp TJ, January CT, Beebe DJ, Microfluidic cell culture and its application in high-throughput drug screening: cardiotoxicity assay for hERG channels, J Biomol Screen 16(1) (2011) 101–11. [PubMed: 21131594]

[19]. Stancescu M, Molnar P, McAleer CW, McLamb W, Long CJ, Oleaga C, Prot JM, Hickman JJ, A phenotypic in vitro model for the main determinants of human whole heart function, Biomaterials 60 (2015) 20–30. [PubMed: 25978005]

[20]. Baillie TA, Rettie AE, Role of biotransformation in drug-induced toxicity: influence of intra-and inter-species differences in drug metabolism, Drug Metab Pharmacokinet 26(1) (2011) 15–29. [PubMed: 20978360]

[21]. NCBI, Terfenadine, in: P.C. Database (Ed.) 2017.

[22]. Das M, Wilson K, Molnar P, Hickman JJ, Differentiation of skeletal muscle and integration of myotubes with silicon microstructures using serum-free medium and a synthetic silane substrate, Nat Protoc 2(7) (2007) 1795–801. [PubMed: 17641647]

[23]. Long C, Finch C, Esch M, Anderson W, Shuler M, Hickman J, Design optimization of liquid-phase flow patterns for microfabricated lung on a chip, Ann Biomed Eng 40(6) (2012) 1255–67. [PubMed: 22271245]

[24]. Natarajan A, Stancescu M, Dhir V, Armstrong C, Sommerhage F, Hickman JJ, Molnar P, Patterned cardiomyocytes on microelectrode arrays as a functional, high information content drug screening platform, Biomaterials 32(18) (2011) 4267–74. [PubMed: 21453966]

[25]. Oleaga C, Bernabini C, Smith AS, Srinivasan B, Jackson M, McLamb W, Platt V, Bridges R, Cai Y, Santhanam N, Berry B, Najjar S, Akanda N, Guo X, Martin C, Ekman G, Esch MB, Langer J, Ouedraogo G, Cotovio J, Breton L, Shuler ML, Hickman JJ, Multi-Organ toxicity demonstration in a functional human in vitro system composed of four organs, Sci Rep 6 (2016) 20030. [PubMed: 26837601]

[26]. Wilson K, Das M, Wahl KJ, Colton RJ, Hickman J, Measurement of contractile stress generated by cultured rat muscle on silicon cantilevers for toxin detection and muscle performance enhancement, PLoS One 5(6) (2010) e11042. [PubMed: 20548775]

[27]. Ayash LJ, Wright JE, Tretyakov O, Gonin R, Elias A, Wheeler C, Eder JP, Rosowsky A, Antman K, Frei E, 3rd, Cyclophosphamide pharmacokinetics: correlation with cardiac toxicity and tumor response, J Clin Oncol 10(6) (1992) 995–1000. [PubMed: 1588381]

[28]. Emadi A, Jones RJ, Brodsky RA, Cyclophosphamide and cancer: golden anniversary, Nat Rev Clin Oncol 6(11) (2009) 638–47. [PubMed: 19786984]

[29]. Goldberg MA, Antin JH, Guinan EC, Rappeport JM, Cyclophosphamide cardiotoxicity: an analysis of dosing as a risk factor, Blood 68(5) (1986) 1114–8. [PubMed: 3533179]

[30]. Nishikawa T, Miyahara E, Kurauchi K, Watanabe E, Ikawa K, Asaba K, Tanabe T, Okamoto Y, Kawano Y, Mechanisms of Fatal Cardiotoxicity following High-Dose Cyclophosphamide Therapy and a Method for Its Prevention, PLoS One 10(6) (2015) e0131394. [PubMed: 26114497]

[31]. Anderson LW, Chen TL, Colvin OM, Grochow LB, Collins JM, Kennedy MJ, Strong JM, Cyclophosphamide and 4-Hydroxycyclophosphamide/aldophosphamide kinetics in patients receiving high-dose cyclophosphamide chemotherapy, Clin Cancer Res 2(9) (1996) 1481–7. [PubMed: 9816324]

[32]. Atalay F, Gulmez O, Ozsancak Ugurlu A, Cardiotoxicity following cyclophosphamidetherapy: a case report, J Med Case Rep 8 (2014) 252. [PubMed: 25023062]

[33]. Dhesi S, Chu MP, Blevins G, Paterson I, Larratt L, Oudit GY, Kim DH, Cyclophosphamide-Induced Cardiomyopathy: A Case Report, Review, and Recommendations for Management, J Investig Med High Impact Case Rep 1(1) (2013) 2324709613480346.

[34]. Guglin M, Aljayeh M, Saiyad S, Ali R, Curtis AB, Introducing a new entity: chemotherapy-induced arrhythmia, Europace 11(12) (2009) 1579–86. [PubMed: 19801562]

[35]. Lushnikova EL, Nepomnyashchikh LM, Sviridov EA, Klinnikova MG, Ultrastructural signs of cyclophosphamide-induced damage to cardiomyocytes, Bull Exp Biol Med 146(3) (2008) 366–71. [PubMed: 19240862]

[36]. Senkus E, Jassem J, Cardiovascular effects of systemic cancer treatment, Cancer Treat Rev 37(4) (2011) 300–11. [PubMed: 21126826]

[37]. Struck RF, Alberts DS, Horne K, Phillips JG, Peng YM, Roe DJ, Plasma pharmacokinetics of cyclophosphamide and its cytotoxic metabolites after intravenous versus oral administration in a randomized, crossover trial, Cancer Res 47(10) (1987) 2723–6. [PubMed: 3552204]

[38]. Conklin DJ, Haberzettl P, Jagatheesan G, Baba S, Merchant ML, Prough RA, Williams JD, Prabhu SD, Bhatnagar A, Glutathione S-transferase P protects against cyclophosphamide-induced cardiotoxicity in mice, Toxicol Appl Pharmacol 285(2) (2015) 136–48. [PubMed: 25868843]

[39]. Chen C, Some pharmacokinetic aspects of the lipophilic terfenadine and zwitterionic fexofenadine in humans, Drugs R D 8(5) (2007) 301–14. [PubMed: 17767395]

[40]. Crumb WJ, Jr., Loratadine blockade of K(+) channels in human heart: comparison with terfenadine under physiological conditions, J Pharmacol Exp Ther 292(1) (2000) 261–4. [PubMed: 10604956]

[41]. Woosley RL, Chen Y, Freiman JP, Gillis RA, Mechanism of the cardiotoxic actions of terfenadine, JAMA 269(12) (1993) 1532–6. [PubMed: 8445816]

[42]. Rampe D, Wible B, Brown AM, Dage RC, Effects of terfenadine and its metabolites on a delayed rectifier K+ channel cloned from human heart, Mol Pharmacol 44(6) (1993) 1240–5. [PubMed: 8264561]

[43]. Yang T, Prakash C, Roden DM, Snyders DJ, Mechanism of block of a human cardiac potassium channel by terfenadine racemate and enantiomers, Br J Pharmacol 115(2) (1995) 267–74. [PubMed: 7670728]

[44]. Eller MG, Walker BJ, Westmark PA, Ruberg SJ, Antony KK, McNutt BE, Okerholm RA, Pharmacokinetics of terfenadine in healthy elderly subjects, J Clin Pharmacol 32(3) (1992) 267–71. [PubMed: 1564131]

[45]. Simpson K, Jarvis B, Fexofenadine: a review of its use in the management of seasonal allergic rhinitis and chronic idiopathic urticaria, Drugs 59(2) (2000) 301–21. [PubMed: 10730552]

[46]. Oleaga C, Legters G, Bridges LR, Kumanchik L, Martin C, Cai Y, Schnepper M, McAleer CW, Long CJ, Hickman JJ, Contractile Force Readout of hESC-Cardiomyocytes, in: Clements M,

Roquemore L (Eds.), Stem Cell-Derived Models in Toxicology, Methods in Pharmacology and Toxicology, Springer Science+Business Media, New York, 2017, pp. 229–246.

[47]. Edwards D, Stancescu M, Molnar P, Hickman JJ, Two cell circuits of oriented adult hippocampal neurons on self-assembled monolayers for use in the study of neuronal communication in a defined system, ACS Chem Neurosci 4(8) (2013) 1174–82. [PubMed: 23611164]

[48]. Smith AS, Long CJ, McAleer C, Bobbitt N, Srinivasan B, Hickman JJ, Utilization of microscale silicon cantilevers to assess cellular contractile function in vitro, J Vis Exp (92) (2014) e51866. [PubMed: 25350792]

[49]. Esch MB, Prot JM, Wang YI, Miller P, Llamas-Vidales JR, Naughton BA, Applegate DR, Shuler ML, Multi-cellular 3D human primary liver cell culture elevates metabolic activity under fluidic flow, Lab Chip 15(10) (2015) 2269–77. [PubMed: 25857666]

[50]. Esch MB, Ueno H, Applegate DR, Shuler ML, Modular, pumpless body-on-a-chip platform for the co-culture of GI tract epithelium and primary liver tissue, Lab Chip 16 (2016) 2719–2729. [PubMed: 27332143]

[51]. Sung JH, Kam C, Shuler ML, A microfludic device for a pharmacokinetic-pharmacodynamic (PK-PD) model on a chip, Lab Chip 10 (2010) 446–455. [PubMed: 20126684]

[52]. Wang YI, Abaci HE, Shuler ML, Microfluidic blood-brain barrier model provides in vivo-like barrier properties for drug permeability screening, Biotechnol Bioeng 114 (2017) 184–194. [PubMed: 27399645]

[53]. Abaci HE, Gledhill K, Guo Z, Christiano AM, Shuler ML, Pumpless Microfluidic platform for drug testing on human skin equivalents, Lab Chip 15 (2015) 882. [PubMed: 25490891]

[54]. Bolleyn J, Rogiers V, Vanhaecke T, Functionality Testing of Primary Hepatocytes in Culture by Measuring Urea Synthesis, Methods Mol Biol 1250 (2015) 317–21. [PubMed: 26272154]

[55]. Nicholson JP, Wolmarans MR, Park GR, The role of albumin in critical illness, Br J Anaesth 85(4) (2000) 599–610. [PubMed: 11064620]

[56]. Prueksaritanont T, Chu X, Gibson C, Cui D, Yee KL, Ballard J, Cabalu T, Hochman J, Drug-drug interaction studies: regulatory guidance and an industry perspective, AAPS J 15(3) (2013) 629–45. [PubMed: 23543602]

[57]. Villeneuve J-P, Pichette V, Cytochrome P450 and Liver Diseases, Current Drug Metabolism 5 (2004) 273– 282. [PubMed: 15180496]

[58]. Guengerich FP, Cytochrome p450 and chemical toxicology, Chem Res Toxicol 21(1) (2008) 70–83. [PubMed: 18052394]

[59]. Ingelman-Sundberg M, Pharmacogenetics of cytochrome P450 and its applications in drug therapy: the past, present and future, Trends Pharmacol Sci 25(4) (2004) 193–200. [PubMed: 15063083]

[60]. Whitlock JP, Jr., Induction of cytochrome P4501A1, Annu Rev Pharmacol Toxicol 39 (1999) 103–25. [PubMed: 10331078]

[61]. Bjornsson TD, Callaghan JT, Einolf HJ, Fischer V, Gan L, Grimm S, Kao J, King SP, Miwa G, Ni L, Kumar G, McLeod J, Obach RS, Roberts S, Roe A, Shah A, Snikeris F, Sullivan JT, Tweedie D, Vega JM, Walsh J, Wrighton SA, R. Pharmaceutical, G. Manufacturers of America Drug Metabolism/Clinical Pharmacology Technical Working, F.D.A.C.f.D. Evaluation, Research, The conduct of in vitro and in vivo drug-drug interaction studies: a Pharmaceutical Research and Manufacturers of America (PhRMA) perspective, Drug Metab Dispos 31(7) (2003) 815–32. [PubMed: 12814957]

[62]. Chu V, Einolf HJ, Evers R, Kumar G, Moore D, Ripp S, Silva J, Sinha V, Sinz M, Skerjanec A, In vitro and in vivo induction of cytochrome p450: a survey of the current practices and recommendations: a pharmaceutical research and manufacturers of america perspective, Drug Metab Dispos 37(7) (2009) 1339–54. [PubMed: 19389860]

[63]. Ogu CC, Maxa JL, Drug interactions due to cytochrome P450, Proc (Bayl Univ Med Cent) 13(4) (2000) 421–3. [PubMed: 16389357]

[64]. Pirozzi KL, Long CJ, McAleer CW, Smith AS, Hickman JJ, Correlation of embryonic skeletal muscle myotube physical characteristics with contractile force generation on an atomic force microscope-based bio-microelectromechanical systems device, Appl Phys Lett 103(8) (2013) 83108. [PubMed: 24046483]

[65]. Muppavarapu R, Guttikar S, Rajappan M, Kamarajan K, Mullangi R, Sensitive LCMS/MS-ESI method for simultaneous determination of montelukast and fexofenadine in human plasma: application to a bioequivalence study, Biomed Chromatogr 28(8) (2014) 1048–56. [PubMed: 24424850]

[66]. Xu A, Linderholm K, Peng L, Hulse J, Development and validation of an LC-MS-MS method for the determination of terfenadine in human plasma, J Pharm Biomed Anal 14(12) (1996) 1675–80. [PubMed: 8887714]

[67]. Rashidi H, Alhaque S, Szkolnicka D, Flint O, Hay DC, Fluid shear stress modulation of hepatocyte-like cell function, Arch Toxicol 90 (2016) 1757–1761. [PubMed: 26979076]

[68]. Tanaka Y, Yamato M, Okano T, Kitamori T, Sato K, Evaluation of effects of shear stress on hepatocytes by a microchip-based system, Measurement Science and Technology 17 (2006) 3167.

[69]. Brown HS, Griffin M, Houston JB, Evaluation of cryopreserved human hepatocytes as an alternative in vitro system to microsomes for the prediction of metabolic clearance, Drug Metab Dispos 35(2) (2007) 293–301. [PubMed: 17132764]

[70]. Rodrigues AD, Mulford DJ, Lee RD, Surber BW, Kukulka MJ, Ferrero JL, Thomas SB, Shet MS, Estabrook RW, In vitro metabolism of terfenadine by a purified recombinant fusion protein containing cytochrome P4503A4 and NADPH-P450 reductase. Comparison to human liver microsomes and precision-cut liver tissue slices, Drug Metab Dispos 23(7) (1995) 765–75. [PubMed: 7587966]

[71]. Uehara S, Yuki Y, Uno Y, Inoue T, Sasaki E, Yamazaki H, Terfenadine t-butyl hydroxylation catalyzed by human and marmoset cytochrome P450 3A and 4F enzymes in livers and small intestines, Xenobiotica (2017) 1–6.

[72]. Takamoto S, Sakura N, Namera A, Yashiki M, Monitoring of urinary acrolein concentration in patients receiving cyclophosphamide and ifosphamide, J Chromatogr B Analyt Technol Biomed Life Sci 806(1) (2004) 59–63.

[73]. Okerholm RA, Weiner DL, Hook RH, Walker BJ, Leeson GA, Biedenbach SA, Cawein MJ, Dusebout TD, Wright GJ, Myers M, Schindler V, Cook CE, Bioavailability of terfenadine in man, Biopharm Drug Dispos 2(2) (1981) 185–90. [PubMed: 6113858]

[74]. Rau SE, Bend JR, Arnold MO, Tran LT, Spence JD, Bailey DG, Grapefruit juice-terfenadine single-dose interaction: magnitude, mechanism, and relevance, Clin Pharmacol Ther 61(4) (1997) 401–9. [PubMed: 9129557]

[75]. Ling KH, Leeson GA, Burmaster SD, Hook RH, Reith MK, Cheng LK, Metabolism of terfenadine associated with CYP3A(4) activity in human hepatic microsomes, Drug Metab Dispos 23(6) (1995) 631–6. [PubMed: 7587944]

[76]. Ortiz de Montellano PR, Cytochrome P450-activated prodrugs, Future Med Chem 5(2) (2013) 213–28. [PubMed: 23360144]

[77]. Toepke MW, Beebe DJ, PDMS absorption of small molecules and consequences in microfluidic applications, Lab Chip 6(12) (2006) 1484–6. [PubMed: 17203151]

[78]. Wang JD, Douville NJ, Takayama S, ElSayed M, Quantitative analysis of molecular absorption into PDMS microfluidic channels, Ann Biomed Eng 40(9) (2012) 1862–73. [PubMed: 22484830]

[79]. van Midwoud PM, Janse A, Merema MT, Groothuis GMM, Verpoorte E, Comparison of Biocompatibility and Adsorption Properties of Different Plastics for Advanced Microfluidic Cell and Tissue Culture Models, Analytical Chemistry 84 (2012) 3938–3944. [PubMed: 22444457]

[80]. Turncliff RZ, Hoffmaster KA, Kalvass JC, Pollack GM, Brouwer KL, Hepatobiliary disposition of a drug/metabolite pair: Comprehensive pharmacokinetic modeling in sandwich-cultured rat hepatocytes, J Pharmacol Exp Ther 318(2) (2006) 881–9. [PubMed: 16690724]

[81]. Li AP, Overview: Evaluation of metabolism-based drug toxicity in drug development, Chem Biol Interact 179(1) (2009) 1–3. [PubMed: 19070611]

[82]. Vunjak-Novakovic G, Bhatia S, Chen C, Hirschi K, HeLiVa platform: integrated heart-liver-vascular systems for drug testing in human health and disease, Stem Cell Res Ther 4 Suppl 1 (2013) S8. [PubMed: 24565063]

[83]. Li AP, Metabolism Comparative Cytotoxicity Assay (MCCA) and Cytotoxic Metabolic Pathway Identification Assay (CMPIA) with cryopreserved human hepatocytes for the evaluation of metabolism-based cytotoxicity in vitro: proof-of-concept study with aflatoxin B1, Chem Biol Interact 179(1) (2009) 4–8. [PubMed: 18950609]

[84]. Li AP, Uzgare A, LaForge YS, Definition of metabolism-dependent xenobiotic toxicity with co-cultures of human hepatocytes and mouse 3T3 fibroblasts in the novel integrated discrete multiple organ co-culture (IdMOC) experimental system: results with model toxicants aflatoxin B1, cyclophosphamide and tamoxifen, Chem Biol Interact 199(1) (2012) 1–8. [PubMed: 22640811]

[85]. Ghanem A, Shuler ML, Combining cell culture analogue reactor designs and PBPK models to probe mechanisms of naphthalene toxicity, Biotechnol Prog 16(3) (2000) 334–45. [PubMed: 10835232]

[86]. Sung JH, Esch MB, Prot JM, Long CJ, Smith A, Hickman JJ, Shuler ML, Microfabricated mammalian organ systems and their integration into models of whole animals and humans, Lab Chip 13(7) (2013) 1201–12. [PubMed: 23388858]

[87]. Tatosian DA, Shuler ML, A novel system for evaluation of drug mixtures for potential efficacy in treating multidrug resistant cancers, Biotechnol Bioeng 103(1) (2009) 187–98. [PubMed: 19137589]

[88]. Imura Y, Yoshimura E, Sato K, Micro total bioassay system for oral drugs: evaluation of gastrointestinal degradation, intestinal absorption, hepatic metabolism, and bioactivity, Anal Sci 28(3) (2012) 197–9. [PubMed: 22451356]

[89]. Kamei K.-i., Kato Y, Hirai Y, Ito S, Satoh J, Oka A, Tsuchiya T, Chen Y, Tabata O, Integrated heart/cancer on a chip to reproduce the side effects of anti-cancer drugs in vitro, RSC Adv 7(58) (2017) 36777–36786.

[90]. Inoue T TK, Mishima M and Watanabe K, Predictive in vitro cardiotoxicity and hepatotoxicity screening system using neonatal rat heart cells and rat hepatocytes, Japanese Society for Alternatives to Animal Experiments 14(6th World Congress on Alternatives & Animal Use in the Life Sciences) (2007) 457–462.

[91]. Rossato LG, Costa VM, de Pinho PG, Arbo MD, de Freitas V, Vilain L, de Lourdes Bastos M, Palmeira C, Remiao F, The metabolic profile of mitoxantrone and its relation with mitoxantrone-induced cardiotoxicity, Arch Toxicol 87(10) (2013) 1809–20. [PubMed: 23545721]

[92]. Baskin KK, Bookout AL, Olson EN, The heart-liver metabolic axis: defective communication exacerbates disease, EMBO Mol Med 6(4) (2014) 436–8. [PubMed: 24623378]

[93]. Glasgow JE, Colman RW, Fibronectin synthesized by a human hepatoma cell line, Cancer Res 44(7) (1984) 3022–8. [PubMed: 6327032]

[94]. Moller S, Dumcke CW, Krag A, The heart and the liver, Expert Rev Gastroenterol Hepatol 3(1) (2009) 51–64. [PubMed: 19210113]

[95]. Rienks M, Papageorgiou AP, Frangogiannis NG, Heymans S, Myocardial extracellular matrix: an ever-changing and diverse entity, Circ Res 114(5) (2014) 872–88. [PubMed: 24577967]

[96]. Wang X, Wu L, Aouffen M, Mateescu MA, Nadeau R, Wang R, Novel cardiac protective effects of urea: from shark to rat, Br J Pharmacol 128(7) (1999) 1477–84. [PubMed: 10602326]

[97]. Ripoll C, Yotti R, Bermejo J, Banares R, The heart in liver transplantation, Journal of Hepatology 54(4) (2011) 810–822. [PubMed: 21145840]

[98]. Harmsen S, Meijerman I, Beijnen JH, Schellens JH, Nuclear receptor mediated induction of cytochrome P450 3A4 by anticancer drugs: a key role for the pregnane X receptor, Cancer Chemother Pharmacol 64(1) (2009) 35–43. [PubMed: 18839173]

[99]. Chen TL, Kennedy MJ, Anderson LW, Kiraly SB, Black KC, Colvin OM, Grochow LB, Nonlinear pharmacokinetics of cyclophosphamide and 4-hydroxycyclophosphamide/aldophosphamide in patients with metastatic breast cancer receiving high-dose chemotherapy followed by autologous bone marrow transplantation, Drug Metab Dispos 25(5) (1997) 544–51. [PubMed: 9152592]

[100]. Kalhorn TF, Ren S, Howald WN, Lawrence RF, Slattery JT, Analysis of cyclophosphamide and five metabolites from human plasma using liquid chromatography-mass spectrometry and gas

chromatography-nitrogen-phosphorus detection, J Chromatogr B Biomed Sci Appl 732(2) (1999) 287–98. [PubMed: 10517350]

[101]. Low JE, Borch RF, Sladek NE, Conversion of 4-hydroperoxycyclophosphamide and 4-hydroxycyclophosphamide to phosphoramide mustard and acrolein mediated by bifunctional catalysis, Cancer Res 42(3) (1982) 830–7. [PubMed: 7059981]

[102]. Nakamae H, Tsumura K, Hino M, Hayashi T, Tatsumi N, QT dispersion as a predictor of acute heart failure after high-dose cyclophosphamide, The Lancet 355(9206) (2000) 805–806.

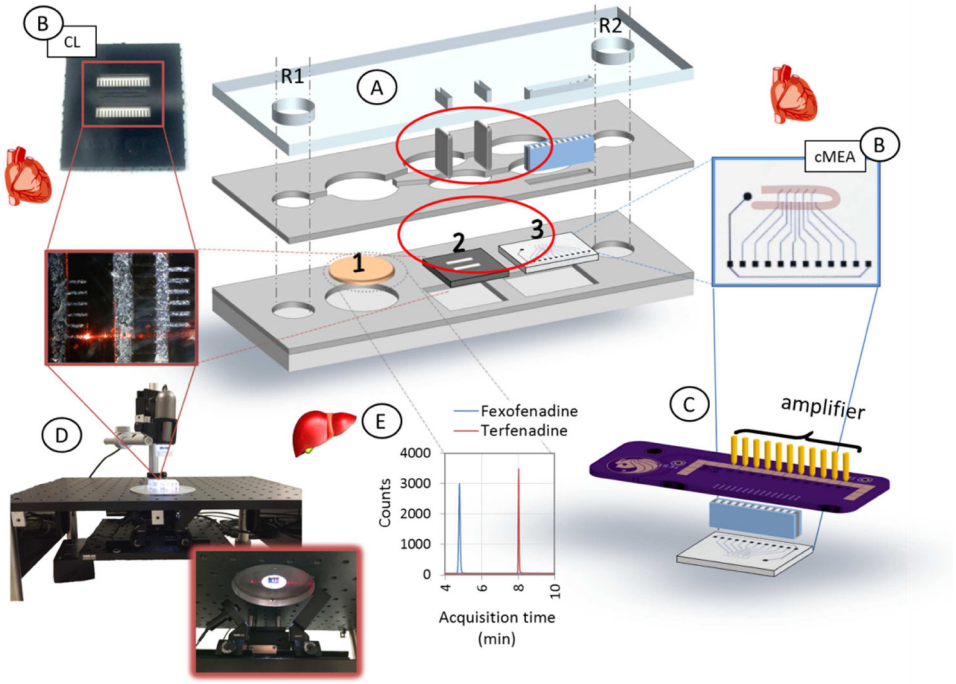

Figure 1. Cardiac and liver co-culture in a pumpless microfluidic system.

A schematic of the microfluidic platform and the interface used to measure the functional activity. Two laser cut acrylic layers housed two laser cut PDMS gaskets that define the microfluidic flow pathway and the compartments for each organ chip (A). Cells were cultured on the respective surfaces: hepatocytes on glass coverslip (compartment 1) and cardiomyocytes on cantilever (compartment 2), and on MEA chips (compartment 3) (A-B). Medium exchange was performed through both reservoirs (R1 and R2), and drug addition through R1. Signals on the MEA chips were recorded utilizing an amplifier via a printed circuit board and an elastomeric connector (C). Cardiac contractile function was measured using a laser-deflection based apparatus (D). Drug compound quantification was performed via HPLC-MS (E).

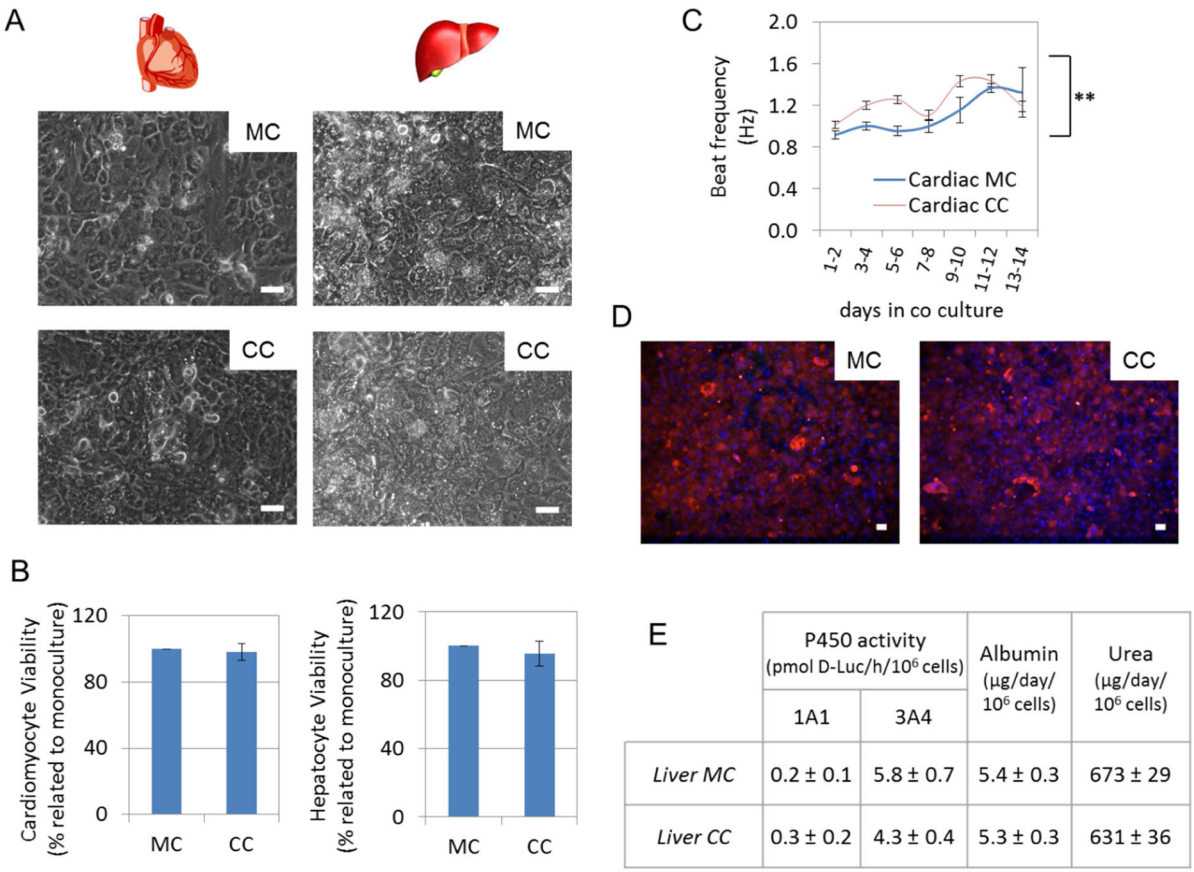

E

	P450 activity (pmol D-Luc/h/10^6 cells)		Albumin (µg/day/ 10^6 cells)	Urea (µg/day/ 10^6 cells)
	1A1	3A4		
Liver MC	0.2 ± 0.1	5.8 ± 0.7	5.4 ± 0.3	673 ± 29
Liver CC	0.3 ± 0.2	4.3 ± 0.4	5.3 ± 0.3	631 ± 36

Figure 2. Characterization of human cardiomyocytes and hepatocytes static co-culture in serum-free medium.

Human iPSc derived cardiomyocytes were co-cultured with human primary hepatocytes in serum-free medium (HSL2, 2 mL) for 7 - 14 days in wells. At day 7, mono-culture (MC; top) or co-culture (CC; bottom) morphology images of cardiomyocytes (A-left) and hepatocytes (A-right), and their viability (p=0.6 and p=0.6, respectively) (B). Spontaneous beat frequency of cardiomyocytes tracked over 14 days of culture appears affected by the time and the presence of the hepatocytes (p=0.002) (C). Albumin (red) and DAPI (blue) staining of hepatocytes at day 7 (D). Hepatocyte albumin (p=0.8) and urea (p=0.4) daily productions, and cytochrome p450 1A1 (p=0.3) and 3A4 (p=0.6) activities at day 7 (E). (50 µm scale). (** p<0.01)

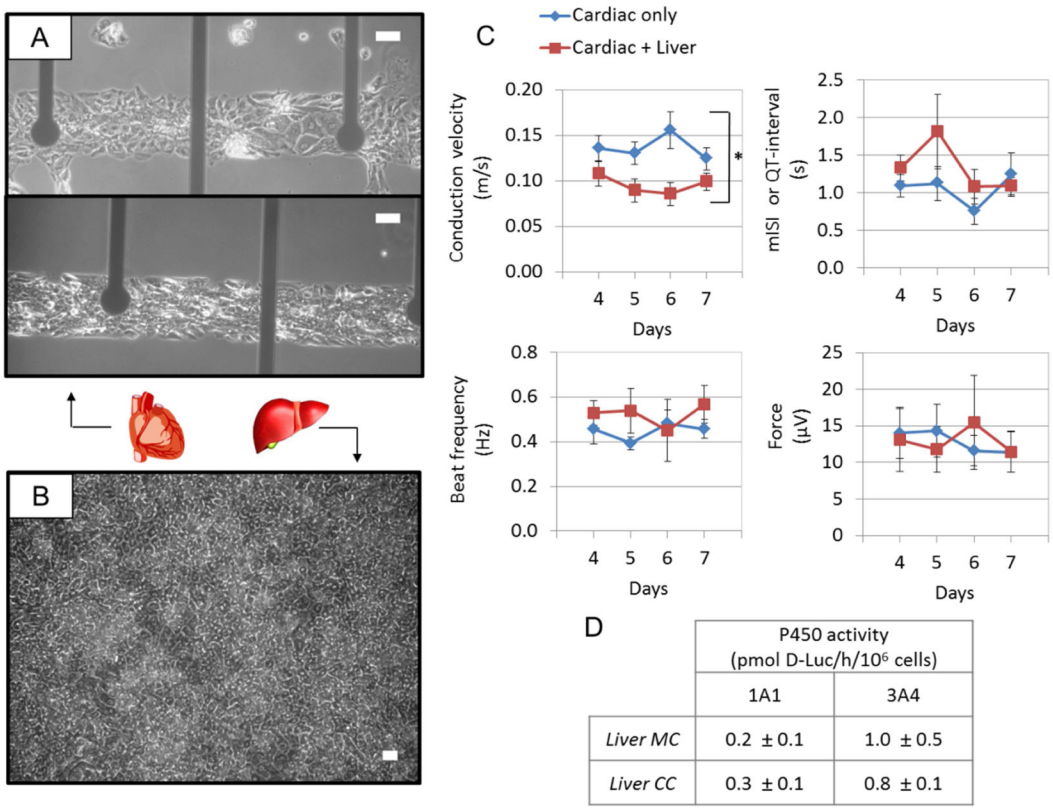

D

	P450 activity (pmol D-Luc/h/10^6 cells)	
	1A1	3A4
Liver MC	0.2 ± 0.1	1.0 ± 0.5
Liver CC	0.3 ± 0.1	0.8 ± 0.1

Figure 3. Characterization of the heart-liver system –serum-free and flow- with non-invasive measurements along seven days.

Human cardiomyocytes and hepatocytes were studied over 7 days in HSL3 medium. Representative morphology images are shown for human cardiomyocytes (A) in mono-culture (top) or co-culture (bottom) (80 μm scale) and hepatocytes in co-culture (B) after 7 days in the housing (50 μm scale). Cardiac function was measured throughout 7 days, in the presence (red square) or absence (blue diamond) of hepatocytes. Cardiac function is plotted as conduction velocity, spontaneous beat frequency, mISI (or QT interval) and contractile force (C). Two-way ANOVA was performed to study the effects of culture time and the presence of the hepatocytes on the different cardiac functional parameters; conduction velocity (p=0.8, 0.03), beat frequency (p=0.8, 0.2), mISI (p=0.3, 0.2) and force (p= 0.7, 0.9). Hepatic function was studied after 7 days in the system with cardiomyocytes and compared to the static mono-culture condition. No significant differences were evident through a t-test for the 1A1 (p=0.09) and 3A4 (p=0.7) enzymes (D).

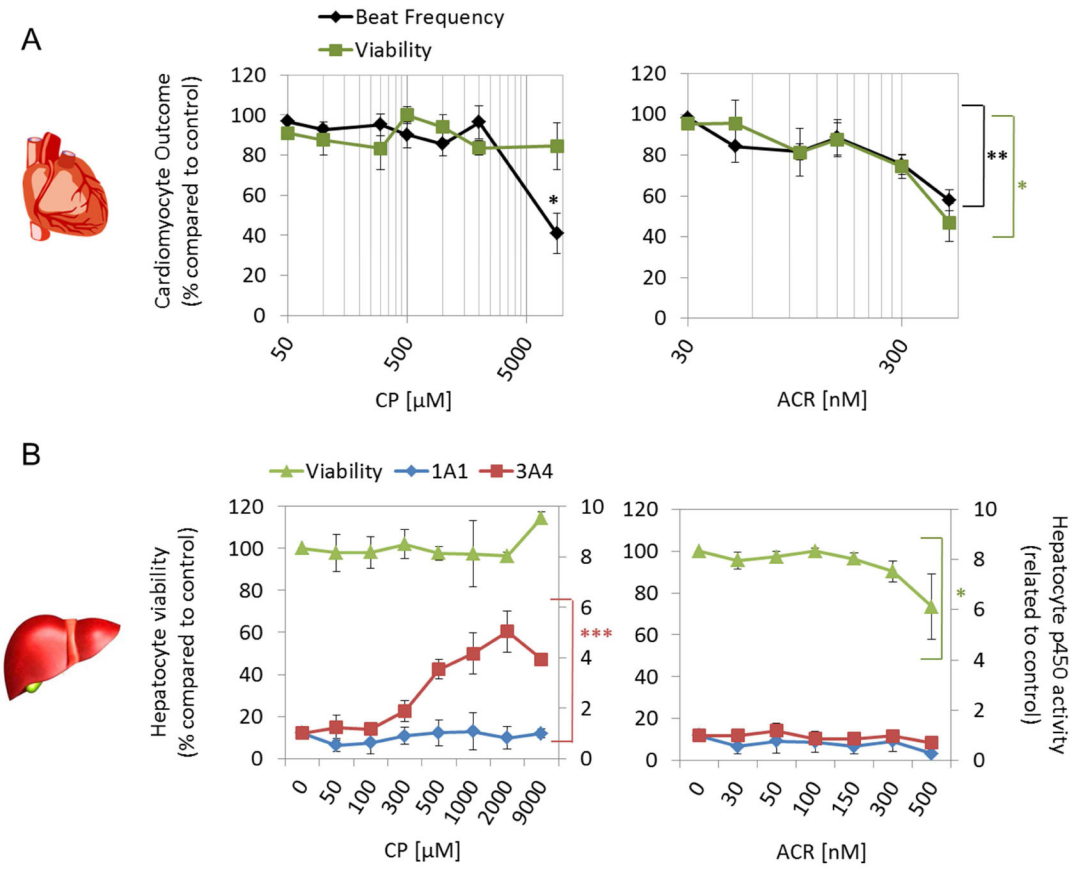

Figure 4. Dose-response of cyclophosphamide and its metabolite acrolein in human cardiomyocytes and hepatocytes.

The viability and function of human cardiomyocytes (A-black diamonds: beat frequency and A-green squares: viability) and hepatocytes (B-blue diamonds: 1A1 activity, B-red squares: 3A4 activity and B-green triangles: viability) in mono-cultures were studied using increasing concentrations of cyclophosphamide (CP; 0-9000 µM) (left) and the metabolite acrolein (ACR; 0-500 nM) (right) for 48 hours in HSL2 medium. The concentrations achieved in the dose-response were studied as a statistical factor influencing cellular function or viability (square brackets). CP reduced beat frequency significantly only at 9000 µM, compared to the control. (* $p<0.05$, ** $p<0.01$; *** $p<0.001$).

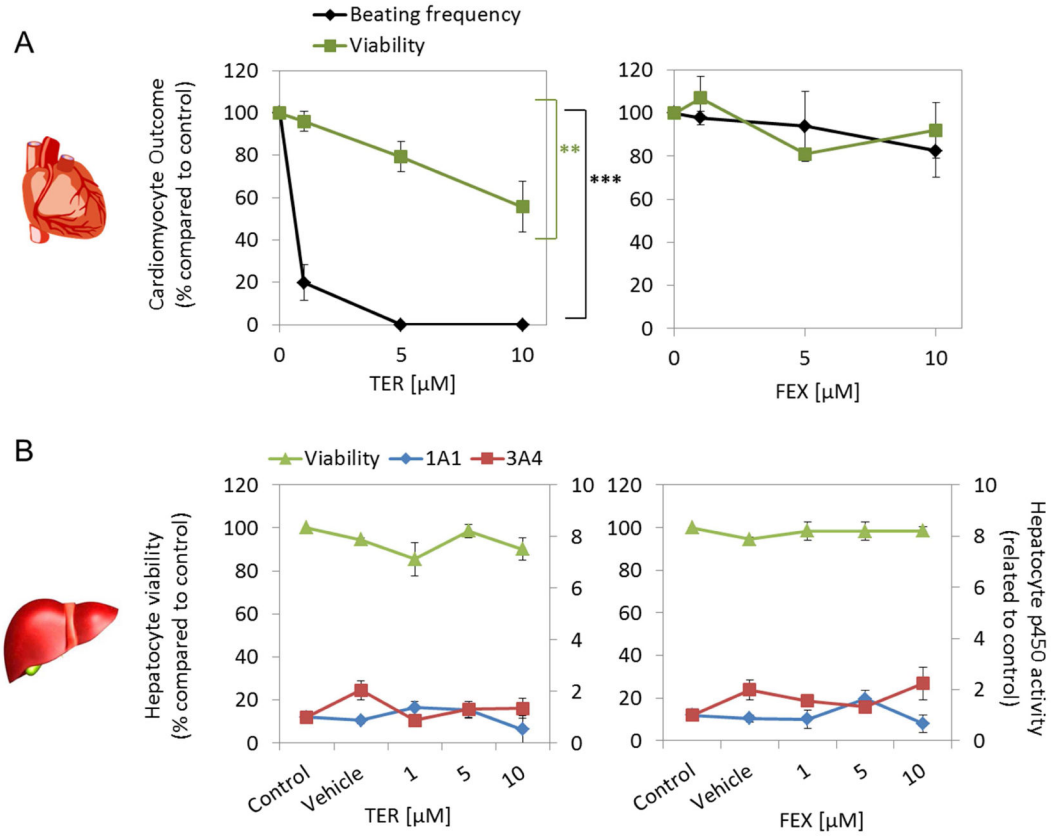

Figure 5. Dose-response of terfenadine and its metabolite fexofenadine in human cardiomyocytes and hepatocytes.

The viability and function of human cardiomyocytes (A-black diamonds: beat frequency and A-green squared: viability) and hepatocytes (B-blue diamonds: 1A1 activity, B-red squares: 3A4 activity and B-green triangles: viability) in mono-cultures upon increasing concentrations of terfenadine (TER; 0-10 µM) (left) and its metabolite fexofenadine (FEX; 0-10 µM) (right) for 48 hours in HSL2 medium. The concentrations achieved in the dose-response were used as a statistical factor influencing cellular function or viability (square brackets). (** $p<0.01$; *** $p<0.001$).

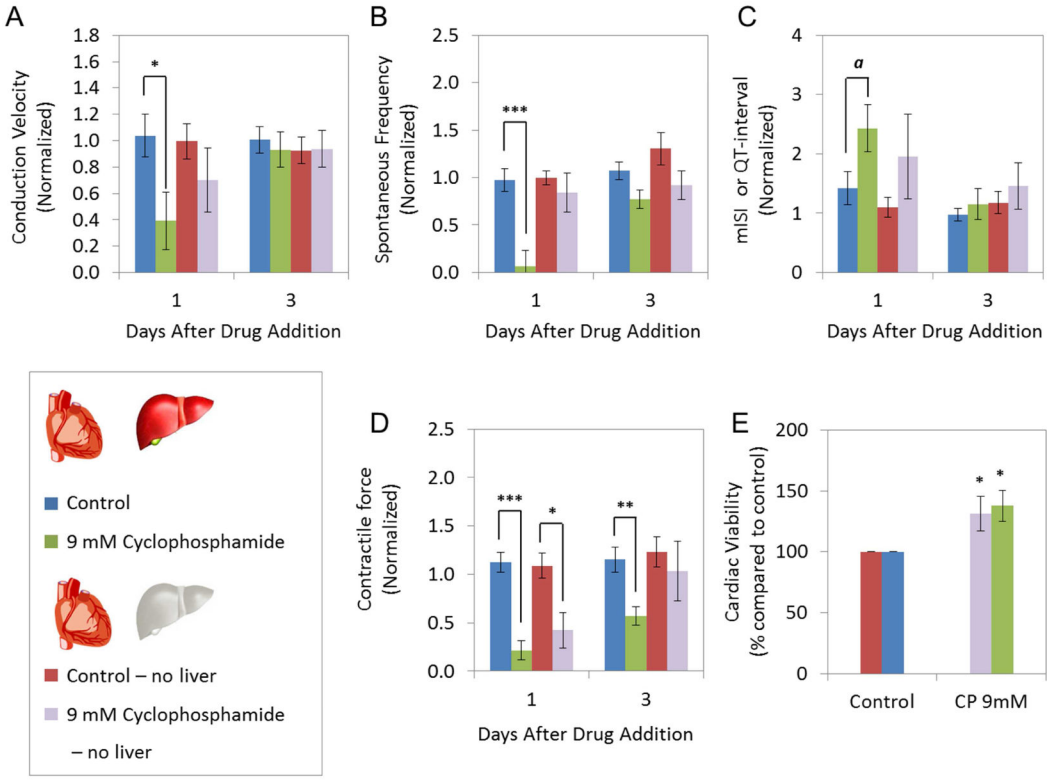

Figure 6. Heart-liver system and cardiac outcome upon cyclophosphamide treatment.

Human iPSc derived cardiomyocytes electrical (A-C) and mechanical (D) activities were evaluated non-invasively before and after 24 and 72 hours of an acute administration of cyclophosphamide (CP, 9 mM), with and without hepatocytes. All values are normalized to the control immediately before drug addition (A-D). As an endpoint analysis, cardiac viability was compared to the control (E). ([a] $p<0.08$, * $p<0.05$, ** $p<0.01$; *** $p<0.001$).

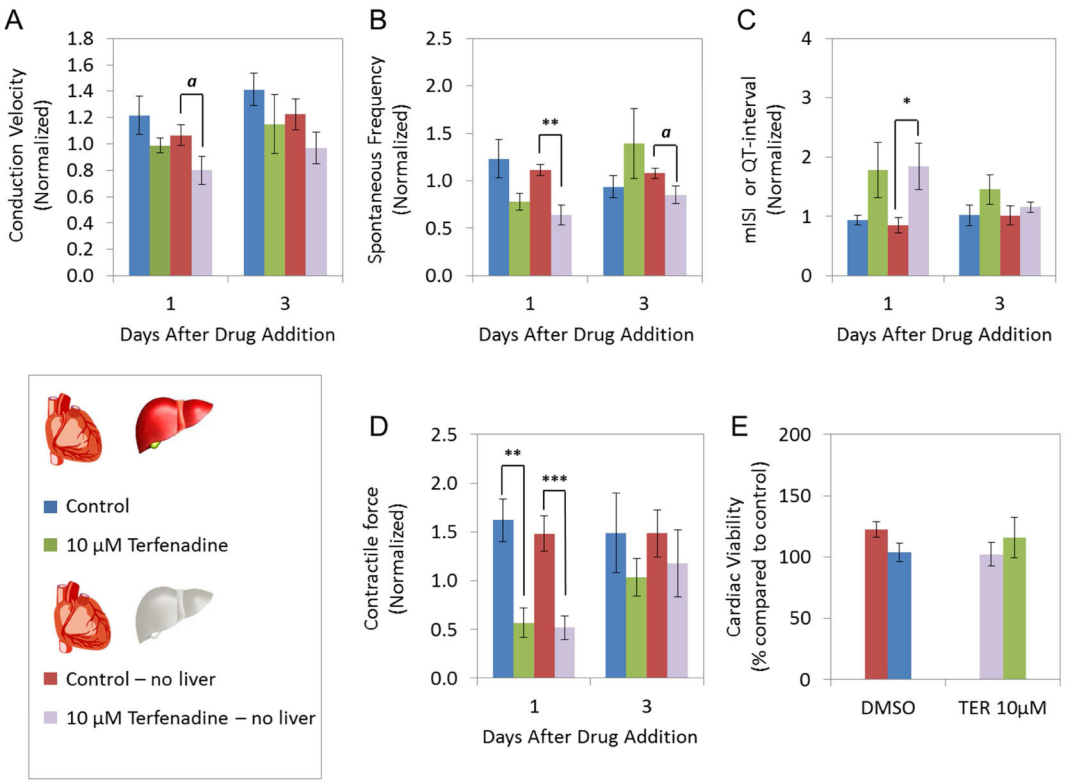

Figure 7. Heart-liver system and cardiac outcome upon terfenadine treatment.

Human iPSc derived cardiomyocytes electrical (A-C) and mechanical (D) activities were evaluated non-invasively after 24 and 72 hours of an acute administration of terfenadine (TER, 10 μM) in the heart-liver system, with and without hepatocytes. All values are normalized to the control immediately before drug addition (A-D). As an endpoint analysis, cardiac viability was compared to the control (E). ([a] $p<0.08$, * $p<0.05$, ** $p<0.01$, *** $p<0.001$).

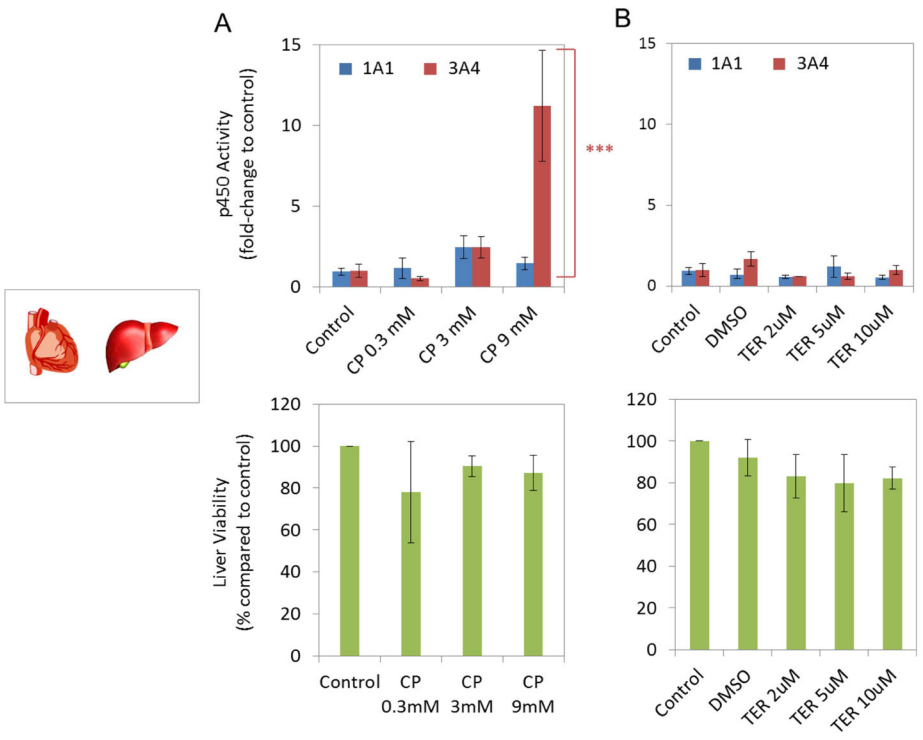

Figure 8. Heart-liver system and hepatic outcome upon drug treatment.

Human primary hepatocytes were evaluated after the acute administration of cyclophosphamide (CP) (A), and terfenadine (TER) (B) in a dose-response fashion. p450 1A1 and 3A4 enzymatic activities (top), and cellular viability (bottom) were analyzed at the endpoint (at day 7, 72 h after drug addition). The concentrations achieved in the dose-response were used as a statistical factor influencing hepatic function and viability (square brackets). (*** $p<0.001$).

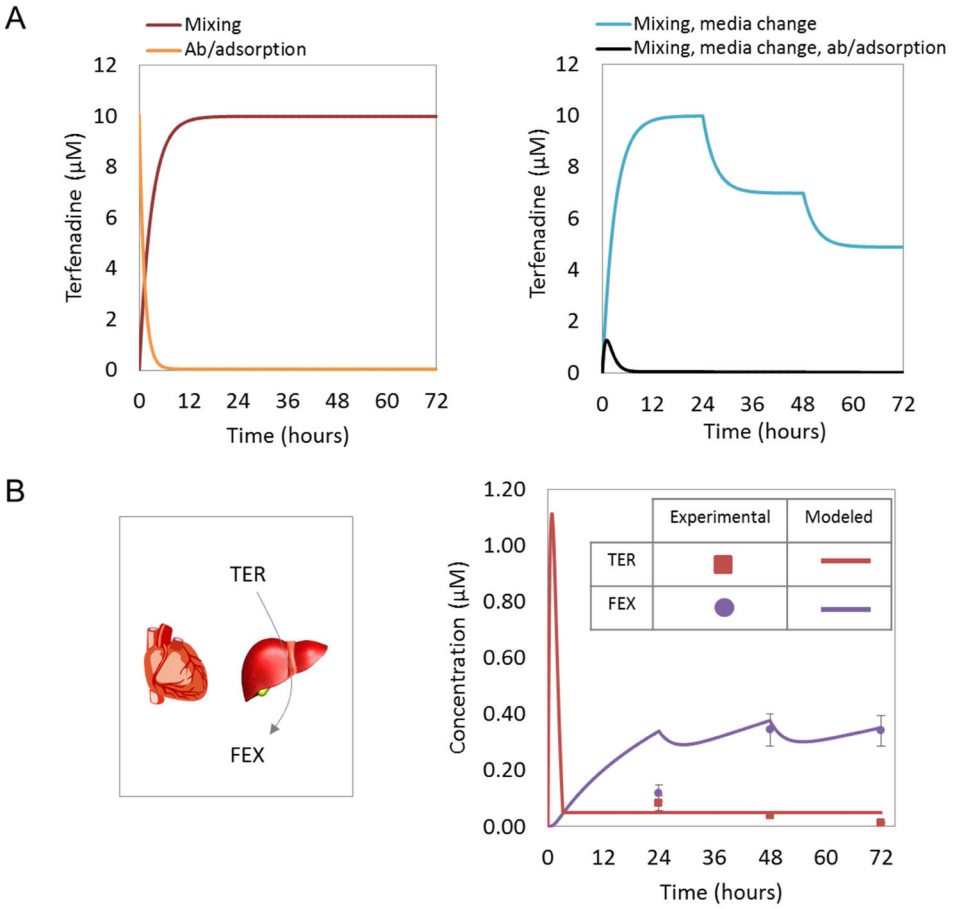

Figure 9. Terfenadine and fexofenadine quantifications and correlation to the pharmacokinetic model.

The predicted concentration of terfenadine in the system over time changes with the system dynamic inputs of mixing, medium change, absorption and adsorption (A). The incorporation of the metabolic input into (A) generates the prediction of terfenadine and fexofenadine concentrations in the system. The experimental quantifications form the heart-liver and the model values are plotted together (B).